# Enumeration of Alkanes as Stereoisomers

Shinsaku Fujita

Department of Chemistry and Materials Technology,

Kyoto Institute of Technology,

Matsugasaki, Sakyoku, Kyoto 606-8585, Japan

E-mail: fujitas@chem.kit.ac.jp

### Abstract

Alkanes are counted as 3D-trees or stereoisomers by means of Fujita's proligand method (S. Fujita, *Theor. Chem. Acc.*, **113**, 73–79, 80–86 (2005); **115**, 37–53 (2006)), where the 3D-trees are categorized into balanced and unbalanced 3D-trees according to the presence or absence of a balance-edge. Such balanced and unbalanced 3D-trees are enumerated by presuming that they are dually recognized as uninuclear and binuclear 3D-trees, where a tetrahedral skeleton of $\mathbf{T}_d$-symmetry is used to generate the uninuclear 3D-trees, while a binuclear skeleton of $\mathbf{D}_{\infty h}$-symmetry is examined to generate the binuclear 3D-trees. The values for binuclear 3D-trees are regarded as contaminants in the enumeration of uninuclear 3D-trees so that the subtraction of the contaminants from the latter enumeration leaves unbalanced 3D-trees to be counted. The enumeration of balanced 3D-trees is conducted directly by using the binuclear skeleton of $\mathbf{D}_{\infty h}$-symmetry. The enumeration is based on functional equations derived from cycle indices with chirality fittingness (CI-CFs), where the functions $a(x^d)$, $c(x^d)$, and $b(x^d)$ (or their modifications) are substituted for three kinds of sphericity indices (SIs), i.e., $a_d$ for homospheric cycles, $c_d$ for enantiospheric cycles, and $b_d$ for hemispheric cycles. Thus, respective functional equations for counting alkanes as well as for itemizing them into achiral and chiral ones are derived by starting from recursive functional equations for counting alkyl ligands as planted 3D-trees. They are programmed by means of the Maple programming language and executed to give respective stereoisomer numbers, which are collected in tabular forms up to carbon content 100.

# 1   Introduction

Pólya's theorem [1, 2] has been widely applied to chemical combinatorics, as described in reviews [3–6] and books [7–11]. However, most works on combinatorial enumeration in chemistry were concerned with constitutional (structural) isomers, which were regarded as graphs in a mathematical context.

After the proposal of the USCI (unit-subduced-cycle-index) approach [12], we have developed various tools for combinatorial enumeration in stereochemistry [13–17], which are capable of treating stereoisomers as three-dimensional (3D) objects. Throughout the development of the tools, we have pointed out the importance of the sphericities of orbits, which are characterized by three kinds of sphericity indices (SIs), i.e., $a_d$ for a homospheric orbit, $c_d$ for an enantiospheric orbit, and $b_d$ for a hemispheric orbit, where the integer $d$ represents the size of the orbit at issue.

As a more simplified version apart from but related implicitly to the USCI approach, we have developed the proligand method for counting stereoisomers, where the sphericities of orbits are modified into the sphericities of cycles [18–21]. One of the merits of Fujita's proligand method is its capability of treating inner structures of molecules in terms of the sphericities of cycles. Thereby, stereochemical problems, such as pseudoasymmetry and *meso*-compounds, are properly treated by Fujita's proligand method in contrast to Pólya's theorem that lacks the sphericity concept.

To the best of our knowledge, one of the most famous problems which were successfully solved by Pólya's theorem is the enumeration of alkanes (equivalently trees) as graph [1, 2]. This problem was first undertaken by Cayley [22, 23], treated more chemically by Henze and Blair [24, 25], and then solved systematically by Pólya [1, 2] and by Otter [26]. Although Robinson et al. [27] reported the enumeration of alkanes as stereoisomers by modifying Pólya's cycle indices (CIs), their treatment did not involve the sphericity concept so that it was incapable of treating pseudoasymmetry and *meso*-compounds properly.

To show the versatility of Fujita's proligand method, the enumeration of alkanes as stereoisomers should be studied in comparison with the enumeration of alkanes as constitutional isomers (graphs) by Pólya's theorem. However, because this study requires a strict mathematical formulation, another practical approach based on personal-computer calculations would be desirable to grasp essential features of Fujita's proligand method.

In order to accomplish the enumeration of alkanes as stereoisomers, the present paper deals with a succinct description of Fujita's proligand method and with the writing and executing of programs for counting them by using the Maple programming language. Thereby, the present paper would involve all of the three elements which *MATCH Commun. Math. Comput. Chem.* aims at.

# 2   Alkyl Ligands as Planted 3D-Trees

Because the present paper aims at counting alkanes, the term *trees* (or *3D-trees*) is mainly used to refer to trees of degree 4 (or 3D-trees of degree 4), where non-terminal vertices mimic carbon atoms of tetravalency. Relevant terms such as *planted 3D-trees* are also used according to this convention.

To enumerate alkanes, we should first enumerate alkyl ligands as their components. It is worthwhile here to provide some comments on Pólya's treatment of this problem. Pólya's

**1**

alkyl ligand

planted 3D-tree

**2**

planted promolecule
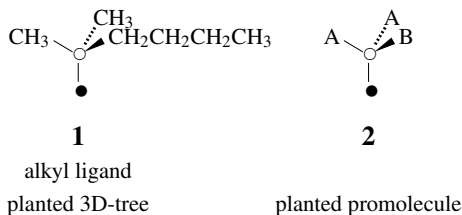
Figure 1: Alkyl ligand (2-methylhex-2-yl ligand) as a planted 3D-tree (**1**) and a planted pro-molecule (**2**). A solid circle (•) represents a root, while an open circle (○) represents a principal node, which is a carbon atom carrying three substitution positions.

treatment, in which alkyl ligands (or planted trees mathematically) are regarded as graphs, has used a cycle index (CI) obtained on the basis of the symmetric group of degree 3 and order 6 ($\mathcal{S}^{[3]}$) as follows [1, 2]:

$$\text{CI}(\mathcal{S}^{[3]}; r_d) = \frac{1}{6}(r_1^3 + 2r_3 + 3r_1 r_2). \tag{1}$$

Let $R_k$ be the number of alkyl ligands of carbon content $k$ (as graphs), which appears as the coefficient of the term $x^k$ in a generating function (an isomer-counting series):

$$r(x) = \sum_{k=0}^{\infty} R_k x^k. \tag{2}$$

According to Pólya's treatment [1, 2], the nested nature of alkyl ligands (as graphs) is charac-terized by the following functional equation:

$$r(x) = 1 + \frac{x}{6}(r(x)^3 + 2r(x^3) + 3r(x)r(x^2)), \tag{3}$$

which is obtained by substituting $r(x^d)$ for the term $r_d$ of the CI (eq. 1). Recursive calculations have been conducted by using eq. 3 [10].

In contrast, Fujita's proligand method [18–21] regards alkyl ligands as 3D-objects, which are mathematically treated as planted 3D-trees or chemically as planted promolecules. For example, a 2-methylhex-2-yl ligand shown in Fig. 1 is regarded mathematically as a planted 3D-tree (**1**), which is chemically regarded as a planted promolecule (**2**), where we put A = $CH_3$ (methyl) and B = $CH_2CH_2CH_2CH_3$ (butyl). Thus, the 2-methylhex-2-yl ligand (**1** as a planted 3D-tree) is constructed by substituting a methyl ligand (A) and a butyl ligand (B) for the three positions of a $\mathbf{C}_{3v}$-skeleton (i.e., the three hydrogens of a methyl ligand as a $\mathbf{C}_{3v}$-skeleton). The nested character of this procedure is found in that the butyl (B) is in turn constructed by substituting one propyl ligand and two hydrogens for the three positions of a $\mathbf{C}_{3v}$-skeleton.

According to Fujita's proligand method [18–21], the three positions of the $\mathbf{C}_{3v}$-skeleton construct an orbit governed by a coset representation (CR), i.e., $\mathbf{C}_{3v}(/\mathbf{C}_s)$. The CR is composed of permutations, each of which is represented by a product of cycles. Each of the cycles is classified into a homospheric, enantiospheric, or hemispheric one, which is characterized by a sphericity index (SI), i.e., $a_d$ for a homospheric cycle, $c_d$ for an enantiospheric cycle, and $b_d$ for a hemispheric cycle, where the integer $d$ represents the length of the cycle at issue. Thereby, the

three positions of the $C_{3v}$-skeleton are characterized by the following cycle index with chirality fittingness (CI-CF):

$$\text{CI-CF}(C_{3v}; a_d, b_d, c_d) = \frac{1}{6}(b_1^3 + 2b_3 + 3a_1c_2) \tag{4}$$

where the chirality fittingness due to each sphericity index controls the transitivity of chiral or achiral ligands. Thus, the SI $a_d$ permits the transitivity among achiral proligands of the same kind; the SI $c_d$ ($d$ is even) permits the transitivity among diploids of the same kind [19], which are defined as ordered sets of achiral proligands or as ordered pairs of enantiomeric proligands; and the SI $b_d$ permits the transitivity among achiral proligands of the same kind or among chiral proligands of the same kind (the same handedness), where the two enantiomers of each pair are treated separately.

In contrast to Pólya's CI (eq. 1), Fujita's CI-CF (eq. 4) assures no recursive nature, because the evaluation of the left-hand side cannot be used in the successive evaluation of the right-hand side of eq. 4. Instead, each component of the right-hand side of eq. 4, i.e., $a_d$, $c_d$, and $b_d$, is expected to have recursive nature, if they are evaluated distinctly. In fact, they can be evaluated as follows:

$$\text{CI-CF}_A(C_{3v}; a_d, c_d) = a_1c_2 \tag{5}$$

$$\text{CI-CF}_D(C_3; c_d) = \frac{1}{3}(c_2^3 + 2c_6) \quad (d: \text{even}) \tag{6}$$

$$\text{CI-CF}(C_3; b_d) = \frac{1}{3}(b_1^3 + 2b_3), \tag{7}$$

where all of them assure recursive nature. Thus, the CI-CF$_A$ (eq. 5) corresponding to $a_d$ is used to count achiral proligands; the CI-CF$_D$ (eq. 6) corresponding to $c_d$ ($d$ is even) is used to count diploids [19], which are defined as ordered sets of achiral proligands or as ordered pairs of enantiomeric proligands; and the CI-CF (eq. 7) corresponding to $b_d$ is used to count achiral proligands and chiral proligands, where the two enantiomers of each pair are counted separately.

Let $\alpha_k$ be the number of achiral alkyl ligands of carbon content $k$ (as stereoisomers); let $\gamma_k$ be the number of diploids [19], which are defined as ordered sets of achiral alkyl ligands or as ordered pairs of enantiomeric alkyl ligands; and let $\beta_k$ be the number of achiral proligands and chiral proligands, where the two enantiomers of each pair are counted separately. Then, suppose that they appear as the coefficients of the term $x^k$ in the following generating functions:

$$a(x) = \sum_{k=0}^{\infty} \alpha_k x^k \tag{8}$$

$$c(x^2) = \sum_{k=0}^{\infty} \gamma_{2k} x^{2k} \tag{9}$$

$$b(x) = \sum_{k=0}^{\infty} \beta_k x^k. \tag{10}$$

By substituting $a(x^d)$, $c(x^d)$, and $b(x^d)$ for the terms $a_d$, $c_d$, and $b_d$ of the CI-CFs (eqs. 5–7), we obtain the following functional equations:

$$a(x) = 1 + xa(x)c(x^2) \tag{11}$$

$$c(x^2) = 1 + \frac{x^2}{3}\{c(x^2)^3 + 2c(x^6)\} \tag{12}$$

$$b(x) = 1 + \frac{x}{3}\{b(x)^3 + 2b(x^3)\}, \tag{13}$$

which can be used in recursive calculations to obtain the coefficients of the generating functions (eqs. 8–10). Note that the multiplication of $x$ for eqs. 11 and 13 and that of $x^2$ for eq. 12 aim at considering the contribution of a principal vertex and the addition of 1 comes from the participation of a null vertex (a hydrogen atom). It should be emphasized that the functional equations (eqs. 11–13) for recursive calculations are concerned with three types of SIs; that is to say, the functional equation $a(x)$ is related to a homospheric cycle via the SI $a_d$, the functional equation $c(x^2)$ is related to an enantiospheric cycle via the SI $c_d$, the functional equation $b(x)$ is related to a hemispheric cycle via the SI $b_d$.

Once we obtain $a(x)$, $c(x^2)$, and $b(x)$ recursively, we are able to obtain $L(x)^{(AC)}$ for counting achiral and chiral ligands, $L(x)^{(A)}$ for counting achiral ligands, and $L(x)^{(C)}$ for counting chiral ligands, where the numbers are itemized with respect to carbon content $k$.

$$L(x)^{(AC)} = \frac{1}{2}(b(x)+a(x)) = 1 + \frac{x}{6}\{b(x)^3 + 2b(x^3) + 3a(x)c(x^2)\} \tag{14}$$

$$L(x)^{(A)} = a(x) = 1 + xa(x)c(x^2) \tag{15}$$

$$L(x)^{(C)} = \frac{1}{2}(b(x)-a(x)) = \frac{x}{6}\{b(x)^3 + 2b(x^3) - 3a(x)c(x^2)\} \tag{16}$$

It should be noted that eq. 14 based on Fujita's proligand method can be transformed into eq. 3 based on Pólya's theorem. Obviously, eq. 3 is a special case of eq. 14 in which we put $r(x) = L(x)^{(AC)}$ in the left-hand side and $r(x) = a(x) = c(x) = b(x)$ in the right-hand side. Because eq. 3 lacks the information on sphericity in contrast to eq. 14, the reverse transformation is impossible.

By replacing $b(x)$ in eq. 10 by $s(x)$, we can obtain a functional equation for counting steric trees,

$$s(x) = 1 + \frac{x}{3}\{s(x)^3 + 2s(x^3)\}, \tag{17}$$

which has the same form as obtained by Pólya's treatment [1, 2]. Note that the combination of eq. 3 and eq. 17 in Pólya's treatment is incapable of characterizing enantiomeric relationships. Obviously, eq. 3 is concerned with graphs or constitutional isomers. The use of eq. 17 results in that one enantiomer and the other enantiomer of each enantiomeric pair are counted separately. In other words, a pair of enantiomers cannot be recognized to exhibit enantiomeric nature during the enumeration of eq. 17.

The sphericity index $b(x)$ of Fujita's proligand method takes account of the difference between achiral and chiral proligands in combination with $a(x)$ and $c(x)$. In contrast, the dummy variables $r(x)$ (eq. 3) and $s(x)$ (eq. 17) of Pólya's treatment implicitly disregards the difference between atoms (or achiral ligands) and chiral ligands in determining geometrical configurations. Although Pólya's theorem was used to discuss the effect of asymmetric carbon atoms [1, 2], it did not properly treated pseudoasymmetric cases and *meso*-compounds.

# 3   Uninuclear and Binuclear 3D-Trees

Trees as graphs and 3D-trees as 3D-objects are composed of vertices and edges. Hence, any tree or 3D-tree is dually characterized by a set of uninuclear trees or 3D-trees and by a set of binuclear trees or 3D-trees. The present section is devoted to clarify the difference between uninuclear 3D-trees and binuclear 3D-trees.

## 3.1 Alkanes as Uninuclear and Binuclear 3D-trees

To emphasize a viewpoint from vertices, we coin the terms *uninucleus* and *binucleus*, which are used to define the terms *uninuclear 3D-trees* and *binuclear 3D-trees*. In particular, we put a focus on the terminal vertices of an edge by using the term *binucleus*. Alkanes as 3D-objects can be dually recognized as uninuclear and binuclear 3D-trees, both of which are constructed by substituting appropriate sets of alkyl ligands, as illustrated in Fig. 2.

Suppose that one vertex (carbon atom) of 2-methylhexane (**3**) is regarded as a uninucleus (•), which is tentatively selected as a special vertex. Then, the alkane of carbon content 7 is expressed by a tetrahedral formula (**4**) having two hydrogens, an isopropyl ligand ($CH(CH_3)_2$), and a propyl ligand ($CH_2CH_2CH_3$). This expression (**4**) is called *a uninuclear 3D-tree*.

When we put $X_1 = CH(CH_3)_2$ and $X_2 = CH_2CH_2CH_3$, we obtain a further simplified formula (**6**), which is called a *uninuclear promolecule*, where the $X_1$ and the $X_2$ regarded as structureless objects with achirality are called *proligands*.
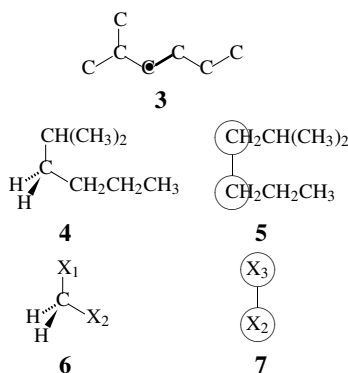


Figure 2: Dual recognition of an alkane (**3**) as a uninuclear (**4**) and a binuclear 3D-tree (**5**), which are further regarded as a uninuclear (**6**) and a binuclear promolecule (**7**).

On the other hand, let us regard one bond of 2-methylhexane (**3**) as a binucleus (marked by a bold line), which we tentatively select as a special edge. Then, the alkane of carbon content 7 is expressed by a pair of dumbbells (**5**) having an isobutyl ligand ($CH_2CH(CH_3)_2$) and a propyl ligand ($CH_2CH_2CH_3$). This expression (**5**) is called *a binuclear 3D-tree*.

When we put $X_3 = CH_2CH_2CH_3$ and $X_2 = CH_2CH(CH_3)_2$, we obtain a further simplified formula (**7**), which is called a *binuclear promolecule*, where the $X_2$ and the $X_3$ regarded as structureless objects with achirality are again called *proligands*.

## 3.2 Enumeration of Uninuclear and Binuclear 3D-Trees

### 3.2.1 Uninuclear 3D-Trees for Evaluating Gross Numbers

To enumerate such uninuclear 3D-trees as **4**, we consider a tetrahedral skeleton (**8**), where the four positions numbered 1 to 4 accommodate a set of proligands. The resulting promolecule is used to determine achirality/chirality. It is further converted into the corresponding 3D-tree by

the subsequent procedure in which the proligands are replaced by ligands (e.g., $X_1 = CH(CH_3)_2$ and $X_2 = CH_2CH_2CH_3$).



**8**          **9**
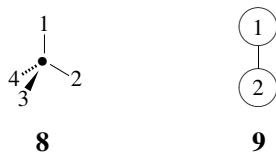
Figure 3: Uninuclear and binuclear skeletons.

Let $G_k^{(AC)}$ be the number of uninuclear 3D-trees of carbon content $k$, where the number of achiral ones and the number of enantiomeric pairs of chiral ones are summed up. Because the number $G_k^{(AC)}$ has a contribution of redundant 3D-trees as exemplified below, it is called the *gross number* of 3D-trees. The gross number $G_k^{(AC)}$ is the coefficient of the term $x^k$ appearing in a generating function:

$$G(x)^{(AC)} = \sum_{k=1}^{\infty} G_k^{(AC)} x^k. \tag{18}$$

Because the uninuclear skeleton (**8**) belongs to $T_d$-symmetry, the four substitution positions are governed by a CR $T_d(/C_{3v})$ according to the USCI approach [12] and the proligand method [18, 19, 20]. Theorem 1 of [20] is applied to this case so as to give the following CI-CF:

$$\text{CI-CF}(T_d; a_d, b_d, c_d) = \frac{1}{24}(b_1^4 + 3b_2^2 + 8b_1 b_3 + 6a_1^2 c_2 + 6c_4), \tag{19}$$

which counts achiral 3D-trees (promolecules) and enantiomeric pairs of chiral 3D-trees (promolecules), where each pair of enantiomers is counted just once.

Let us consider the substitution of the alkyl ligands (the planted promolecules) which have been counted by eqs. 8–10 (eqs. 11–13). This means the replacement of $a_d$, $c_d$, and $b_d$ by $a(x^d)$, $c(x^d)$, and $b(x^d)$, which converts eq. 19 into the following functional equation:

$$G(x)^{(AC)} = \frac{x}{24}\{b(x)^4 + 3b(x^2)^2 + 8b(x)b(x^3) + 6a(x)^2 c(x^2) + 6c(x^4)\}. \tag{20}$$

where the variable $x$ is multiplied to evaluate the central carbon atom of the tetrahedral skeleton (**8**).

Although the gross number of alkanes evaluated by $G(x)^{(AC)}$ (eq. 20) is concerned with uninuclear 3D-trees (promolecules) of each carbon content $k$, it suffers from some redundancy. For example, 2-methylhexane (**3**) shown in Fig. 2 is otherwise regarded as a tetrahedral skeleton having two methyl ligands ($CH_3$) and one butyl ligand ($CH_2CH_2CH_2CH_3$). This contributes to the enumeration result of $G(x)^{(AC)}$ as a redundant 3D-tree (i.e., a contaminant), because it is not congruent with the 3D-tree (**4**) under the action of the point group $T_d$. Because the point group $T_d$ is incapable of determining the congruence between them, we should develop an alternative way to exclude the redundancy after discussing binuclear 3D-trees below.

### 3.2.2  Binuclear 3D-Trees for Evaluating Contaminants

To enumerate such binuclear 3D-trees as **5**, we consider a binuclear skeleton (**9**), where the two positions 1 and 2 accommodate a set of proligands. The resulting promolecule is used to determine achirality/chirality. It is further converted into the corresponding 3D-tree by the subsequent procedure in which the proligands are replaced by ligands (e.g., $X_3 = CH_2CH(CH_3)_2$ and $X_2 = CH_2CH_2CH_3$).

Let $C_k^{(AC)}$ be the number of binuclear 3D-trees (promolecules) of carbon content $k$, where the number of achiral ones and the number of enantiomeric pairs of chiral ones are summed up. The number $C_k^{(AC)}$ is the coefficient of the term $x^k$ appearing in a generating function:

$$C(x)^{(AC)} = \sum_{k=1}^{\infty} C_k^{(AC)} x^k. \tag{21}$$

Because the binuclear skeleton (**9**) belongs to $\mathbf{D}_{\infty h}$-symmetry, the two substitution positions are governed by a CR $\mathbf{D}_{\infty h}(/\mathbf{C}_{\infty v})$, which is isomorphic to a CR $\mathbf{C}_{2v}(/\mathbf{C}_s)$, inclusive of the sphericities of relevant cycles [18–20]. Theorem 1 of [20] is applied to this case so as to give the following CI-CF:

$$\text{CI-CF}(\mathbf{D}_{\infty h}; a_d, b_d, c_d) = \frac{1}{4}(b_1^2 + b_2 + a_1^2 + c_2), \tag{22}$$

which counts achiral 3D-trees (promolecules) and enantiomeric pairs of chiral 3D-trees (promolecules), where each pair of enantiomers is counted just once.

Let us consider the substitution of the alkyl ligands (the planted promolecules) which have been counted by eqs. 8–10 (eqs. 11–13). This procedure means the replacement of $a_d$, $c_d$, and $b_d$ by $a(x^d) - 1$, $c(x^d) - 1$, and $b(x^d) - 1$, where the first term 1 ($x^0$) is subtracted from each of eqs. 11–13, because a null vertex (a hydrogen atom) is not permitted. Thereby, eq. 22 is converted into the following functional equation:

$$C(x)^{(AC)} = \frac{1}{4}\{(b(x) - 1)^2 + (b(x^2) - 1) + (a(x) - 1)^2 + (c(x^2) - 1)\}. \tag{23}$$

## 4  Balanced and Unbalanced 3D-Trees

### 4.1  New Dichotomy for Classifying 3D-Trees

As shown in Subsection 3.2, the number of alkanes (3D-trees) evaluated by $G(x)^{(AC)}$ (eq. 20) is contaminated by redundant uninuclear 3D-trees. The aim of this section is to show that such contaminants can be evaluated by the numbers of binuclear 3D-trees. These are in turn evaluated by $C(x)^{(AC)}$ (eq. 23), as shown in Fig. 4. For the purpose of evaluating such contaminants, we shall examine the subtraction $G(x)^{(AC)} - C(x)^{(AC)}$ in detail.

There are two cases in the evaluation of the subtraction represented by $G(x)^{(AC)} - C(x)^{(AC)}$, so that we shall propose a new dichotomy between balanced 3D-trees and unbalanced 3D-trees. This dichotomy is more essential to evaluate the subtraction than the two conventional dichotomies reported by Jordan [28], i.e., the dichotomies between central and bicentral trees and between centroidal and bicentroidal trees, even if these are extended to cover 3D-trees.

To introduce the new dichotomy, we shall first define a balance-edge. A *balance-edge* is defined as an edge of which two terminals accommodate planted 3D-trees (planted promolecules)
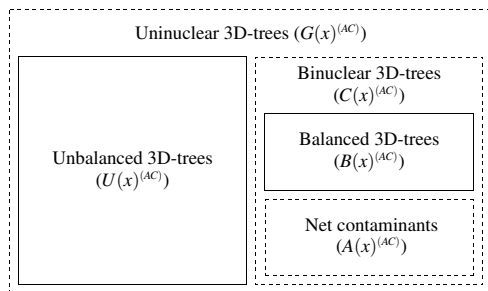
Figure 4: The dichotomy of balanced/unbalanced 3D-trees and the dual recognition as un-iuclear 3D- trees and binuclear 3D-trees. The total number of trees is obtained by summing up the number of unbalanced 3D-trees and the the number of balanced 3D-trees, i.e., $N(x)^{(AC)} = U(x)^{(AC)} + B(x)^{(AC)}$.

congruent under symmetry operations. This means that the two half branches generated by deleting the balance-edge are of the same kind or of an enantiomeric relationship. Obviously, any 3D-tree has at most one balance-edge. That is to say, any 3D-tree contains zero or one balance-edge. Thereby, 3D-trees are classified into two categories: *balanced 3D-trees* with a balance-edge and *unbalanced 3D-trees* with no balance-edge.

The present methodology based on the dichotomy between balanced trees and unbalanced trees as well as on the dual recognition as uninuclear trees and binuclear trees provides us a succinct foundation for understanding the mechanism of enumerating 3D-trees. The relationship between the new terms coined in the present methodology is summarized in Fig. 4.

## 4.2 Enumeration of Unbalanced Trees

### 4.2.1 Full Cancellation of Balanced 3D-Trees

The effect of a balanced tree on the enumeration result by $G(x)^{(AC)}$ is shown in Fig. 5, where the boldfaced edge of a balanced tree **10** is a balance-edge, which is differentiated from other edges called *slant-edges*. In the evaluation of **10** by $G(x)^{(AC)}$, each vertex (carbon atom) can be selected as the central atom of the tetrahedral skeleton (**8**). When we select vertices (○) other than the terminals (●) of the balance-edge, we obtain the formulas shown as **11**–**16**, which are not congruent under $\mathbf{T}_d$-symmetry. Once we select **10** as a 3D-tree to be counted, the uninuclear 3D-trees (**11**–**16**) are regarded as contaminants to be excluded.

Let us alternatively regard the uninuclear 3D-trees (**11**–**13**) as binuclear 3D-trees, where the boldfaced edges (slant-edges) are taken into consideration. Note that each of the boldfaced edges corresponds to each of the vertices (○) selected for evaluating the uninuclear 3D-trees (**11**–**13**). It follows that each of the uninuclear 3D-trees (**11**–**13** with a nucleus represented by the symbol ○) corresponds to each of the binuclear 3D-trees (**11**–**13** with a binucleus represented by a boldfaced edge).

By examining each of the 3D-trees (**11**–**13**) as a binuclear 3D-tree, the ligand at the right-handed terminal contains the balance-edge selected for **10**. Such a ligand as containing a balance-edge is called a *superior ligand*. Once we select **10** as a 3D-tree to be counted, each
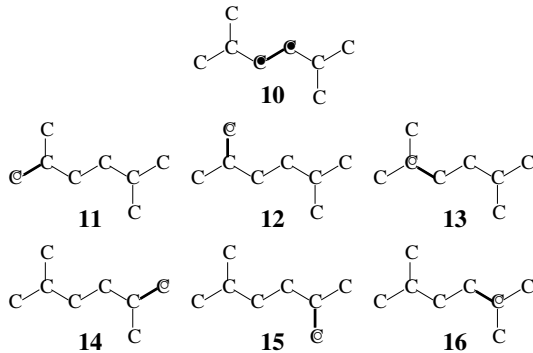
Figure 5: Balanced 3D-tree. Cancellation between uninuclear 3D-trees and binuclear 3D-trees leaves no balanced 3D-tree.

superior ligand can be regarded as being fixed. This condition means that the enumeration as uninuclear 3D-trees is the same thing as the enumeration as binuclear 3D-trees. Hence, cancellation for the 3D-trees (**11–13**) occurs so that the subtraction $G(x)^{(AC)} - C(x)^{(AC)}$ does not contain the 3D-trees (**11–13**).

This discussion holds true for the 3D-trees (**14–16**), which are dually recognized as uninuclear and binuclear 3D-trees. Note that the 3D-trees (**14–16**) are based on the right-half branch, while the 3D-trees (**11–13**) are based on the left-half branch.

Let us then examine the balanced 3D-tree (**10**) to be counted. A set of the two terminal vertices of a balance-edge is called a *twin-core* in order to emphasize a viewpoint of vertices. Note that a balanced-edge is regarded as a special binucleus, which is in turn recognized to be a twin-core from a viewpoint of vertices. The two terminal vertices characterized by the twin-core are equivalent so that it is sufficient to treat either one as a special uninucleus. In this meaning, the term *twin-core* for balanced 3D-trees corresponds to the term *core* for unbalance 3D-trees.

The enumeration of uninuclear 3D-trees by adopting the *left-handed* terminal (•) of the twin-core (i.e., the balance-edge) as a uninucleus gives the result represented by $G(x)^{(AC)}$. On the same line, the enumeration of uninuclear 3D-trees by adopting the *right-handed* terminal (•) of the twin-core as a uninucleus also gives the result represented by $G(x)^{(AC)}$. Note that these results are identical with each other even under the point group $\mathbf{T}_d$, because of the equivalence of the two terminals.

On the other hand, the enumeration of binuclear 3D-trees by adopting the balance-edge (•—•) as a binucleus gives the result represented by $C(x)^{(AC)}$. This enumeration has the same effect as that of $G(x)^{(AC)}$ with respect to the balanced 3D-tree (**10**). Hence, the cancellation for the 3D-tree (**10**), which is dually recognized to be a uninuclear and a binuclear tree, takes place so that the subtraction $G(x)^{(AC)} - C(x)^{(AC)}$ does not contain the 3D-tree (**10**).

Concretely speaking, the balanced 3D-tree (**10**) recognized by $G(x)^{(AC)}$ is a uninuclear 3D-tree having an isopropyl ligand (–CH(CH$_3$)$_2$), an isobutyl ligand (–CH$_2$CH(CH$_3$)$_2$), and two hydrogens, i.e., isopropylisobutylmethane. On the other hand, the balanced 3D-tree (**10**) recognized by $C(x)^{(AC)}$ is a binuclear 3D-tree having two isobutyl lingands, i.e., biisobutyl. Hence,

the cancellation mechanism for the 3D-tree (**10**) stems from the fact that the isopropylisobutyl-methane by $G(x)^{(AC)}$ and the biisobutyl by $C(x)^{(AC)}$ represent the same balanced 3D-tree (**10**).

When a tree or 3D-tree has $v$ vertices and $e$ edges, it satisfies the relationship $v = e + 1$ in general. The discussion for Fig. 5 is based on the modified relationship $v - 2 = e - 1$, where the subtrahend 2 in the left-hand side ($v - 2$) corresponds to the twin-core of the 3D-tree (**10**), while the subtrahend 1 in the right-hand side ($e - 1$) corresponds to the balance-edge of the 3D-tree (**10**). As a result, the right-hand side ($e - 1$) indicates the number of slant-edges in the balanced 3D-tree (**10**). Remember the correspondence between a twin-core from a viewpoint of vertices and a balance-edge from a viewpoint of edges.

Consequently, the cancellation between uninuclear 3D-trees and binuclear 3D-trees leaves no balanced 3D-tree, as shown in Fig. 5. This cancellation holds true for any balanced 3D-trees so that the subtraction $G(x)^{(AC)} - C(x)^{(AC)}$ does not contain balanced 3D-trees in general (cf. Fig. 4).

### 4.2.2 Partial Cancellation of Unbalanced 3D-Trees

The effect of an unbalanced tree on the enumeration result by $G(x)^{(AC)}$ is exemplified in Fig. 6, where there is no balanced edge. Let us select an unbalanced 3D-tree (**3**) to be counted. In the evaluation of **3** by $G(x)^{(AC)}$, however, each vertex (carbon atom) can be selected as the central atom of the tetrahedral skeleton (**8**). When we select vertices (○) other than the core (●) of **3**, we obtain the formulas shown as **17–22**. Once we select **3** as a 3D-tree to be counted, the uninuclear 3D-trees (**17–22**) are regarded as contaminants to be excluded. Note that each of the uninuclear 3D-trees (**17–22**) is not congruent to the 3D-tree (**3**) under the action of $\mathbf{T}_d$.
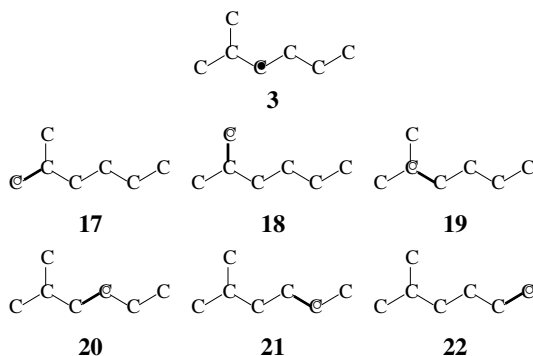


Figure 6: Unbalanced 3D-tree. Cancellation between uninuclear 3D-trees and binuclear 3D-trees leaves an unbalanced 3D-tree (**3**).

By examining each of the 3D-trees (**17–22**) as a binuclear 3D-tree, we take account of a boldfaced edge incident to each uninucleus (○), where the other terminal vertex of the boldfaced edge accommodates a ligand containing the core (●) of **3**. Such a ligand as containing a balance-edge is called a *superior ligand* for an unbalanced 3D-tree. Because the presence of such a superior ligand means that the edge at issue is not balanced, it is called a *slant-edge*. Once we select **3** as a 3D-tree to be counted, each superior ligand can be regarded as being fixed. On the

same line as pointed out in the discussions for Fig. 5, this condition means that the enumeration as uninuclear 3D-trees is the same thing as the enumeration as binuclear 3D-trees. Hence, the cancellation of the 3D-trees (**17–22**) takes place so that the subtraction $G(x)^{(AC)} - C(x)^{(AC)}$ cancels the 3D-trees (**17–22**) out, but leaves **3** as an unbalanced 3D-tree to be counted.

The discussion for Fig. 6 is based on the relationship $v - 1 = e$, which holds true for trees or 3D-trees in general. The subtrahend 1 in the left-hand side ($v - 1$) corresponds to the core of the 3D-tree (**3**). No subtrahend in the right-hand side ($e$) implies that the 3D-tree (**3**) has no balance-edge. As a result, the right-hand side ($e$) indicates the number of slant-edges in the unbalanced 3D-tree (**3**).

It should be noted that the retained unbalanced 3D-tree (**3**) is uniquely determined because the core (●) can be selected to be identical with its centroid or with either one vertex of its bicenter. In general, such a core (●) in an unbalanced 3D-tree can be selected to be identical with a centroid or either one vertex of its bicentroid; or with a center or either one vertex of its bicenter. The selection of such a core is assured by the dichotomy of centroidal and bicentroidal 3D-trees or by the dichotomy of central and bicentral 3D-trees.

### 4.2.3 Unbalanced 3D-Trees as Residual 3D-Trees

The discussions developed for balanced 3D-trees (Fig. 5) and unbalanced 3D-trees (Fig. 6) show that the subtraction $G(x)^{(AC)} - C(x)^{(AC)}$ leaves unbalanced 3D-trees to be counted. See Fig. 4.

Let $U_k^{(AC)}$ be the number of unbalanced 3D-trees of carbon content $k$, where the number of achiral ones and the number of enantiomeric pairs of chiral ones are summed up. The number $U_k^{(AC)}$ is the coefficient of the term $x^k$ appearing in a generating function:

$$U(x)^{(AC)} = \sum_{k=1}^{\infty} U_k^{(AC)} x^k. \tag{24}$$

This generating function is evaluated by the following relationship:

$$U(x)^{(AC)} = G(x)^{(AC)} - C(x)^{(AC)}. \tag{25}$$

Because of eq. 20 for $G(x)^{(AC)}$ and eq. 23 for $C(x)^{(AC)}$, eq. 25 is converted into a functional equation:

$$\begin{aligned} U(x)^{(AC)} &= \frac{x}{24}\{b(x)^4 + 3b(x^2)^2 + 8b(x)b(x^3) + 6a(x)^2 c(x^2) + 6c(x^4)\} \\ &\quad - \frac{1}{4}\{(b(x) - 1)^2 + (b(x^2) - 1) + (a(x) - 1)^2 + (c(x^2) - 1)\}. \end{aligned} \tag{26}$$

By using the coefficients of $G(x)^{(AC)}$ and $C(x)^{(AC)}$, we obtain the following relationship:

$$U_k^{(AC)} = G_k^{(AC)} - C_k^{(AC)}, \tag{27}$$

where the right-hand side is derived by using $G_k^{(AC)}$ (eq. 18) and $C_k^{(AC)}$ (eq. 21).

## 4.3 Enumeration of Balanced 3D-Trees

Let $B_k^{(AC)}$ be the number of balanced 3D-trees of carbon content $k$, where the number of achiral ones and the number of enantiomeric pairs of chiral ones are summed up. The number $B_k^{(AC)}$ is

the coefficient of the term $x^k$ appearing in a generating function:

$$B(x)^{(AC)} = \sum_{k=1}^{\infty} B_k^{(AC)} x^k. \tag{28}$$

Because a balanced 3D-tree is regarded as a symmetric uninuclear 3D-tree (promolecule), it has a set of two achiral ligands of the same kind (A—A), a set of two chiral ligands of the same kind (p—p/$\bar{\text{p}}$—$\bar{\text{p}}$), or a pair of enantiomeric ligands (p—$\bar{\text{p}}$). In order to satisfy these modes of chirality fittingness, the terms $b_2$ and $c_2$ are selected among the terms contained in the right-hand side of eq. 22 so as to give the following CI-CF:

$$\text{CI-CF}_S(\mathbf{D}_{\infty h}; b_d, c_d) = \frac{1}{4}(b_2 + c_2), \tag{29}$$

which counts achiral balanced 3D-trees (promolecules) and enantiomeric pairs of chiral balanced 3D-trees, where each pair of enantiomers is counted just once.

Let us consider the derivation of balanced 3D-trees by the substitution of the alkyl ligands (the planted promolecules) which have been counted by eqs. 8–10 (eqs. 11–13). This procedure means the replacement of $c_d$ and $b_d$ by $c(x^d) - 1$ and $b(x^d) - 1$, where the first term 1 ($x^0$) is subtracted from each of eqs. 11–13, because a null vertex (a hydrogen atom) is not permitted. Thereby, eq. 29 is converted into the following functional equation:

$$B(x)^{(AC)} = \frac{1}{2}\{(b(x^2) - 1) + (c(x^2) - 1)\}. \tag{30}$$

By combining eq. 30 with eq. 23, net contaminants are evaluated by the following functional equation:

$$
\begin{aligned}
A(x)^{(AC)} &= C(x)^{(AC)} - B(x)^{(AC)} \\
&= \frac{1}{4}\{(b(x) - 1)^2 - (b(x^2) - 1) + (a(x) - 1)^2 - (c(x^2) - 1)\}.
\end{aligned}
\tag{31}
$$

## 4.4   Enumeration of 3D-Trees

Let $N_k^{(AC)}$ be the total number of 3D-trees of carbon content $k$, where the number of achiral ones and the number of enantiomeric pairs of chiral ones are summed up. The number $N_k^{(AC)}$ is the coefficient of the term $x^k$ appearing in a generating function:

$$N(x)^{(AC)} = \sum_{k=1}^{\infty} N_k^{(AC)} x^k. \tag{32}$$

The generating function can be evaluated by summing up $U(x)^{(AC)}$ and $B(x)^{(AC)}$ or by subtracting $A(x)^{(AC)}$ from $G(x)^{(AC)}$. By summing up eq. 26 and eq. 30, we obtain the following functional equation:

$$
\begin{aligned}
N(x)^{(AC)} &= G(x)^{(AC)} - A(x)^{(AC)} \\
&= U(x)^{(AC)} + B(x)^{(AC)} \\
&= \frac{x}{24}\{b(x)^4 + 3b(x^2)^2 + 8b(x)b(x^3) + 6a(x)^2 c(x^2) + 6c(x^4)\} \\
&\quad - \frac{1}{4}\{(b(x) - 1)^2 - (b(x^2) - 1) + (a(x) - 1)^2 - (c(x^2) - 1)\},
\end{aligned}
\tag{33}
$$

which gives the total number of 3D-trees of carbon content $k$ as the coefficient of the term $x^k$.

## 4.5   Implementation of a Program for Counting 3D-Trees

The functional equations $U(x)^{(AC)}$ (eq. 26), $B(x)^{(AC)}$ (eq. 30), and $N(x)^{(AC)}$ (eq. 33) are programmed by means of the Maple programming language to give the following code, which is stored in a file named "NUB-AC1-100.mpl" tentatively.

A Maple program for counting alkanes, "NUB-AC1-100.mpl":

```
"Functional Equations for Alkyl Ligands";
ax := 1 + x*a1*c2;
cx := 1+ (1/3)*x^2*c2^3 + (2/3)*x^2*c6;
bx := 1 + (1/3)*x*b1^3 + (2/3)*x*b3;

"Initial Values";
a1 := 1; a2 := 1;
b1 := 1; b2 := 1; b3 := 1;
c2 := 1; c4 := 1; c6 := 1;

"Recursive Calculation";
for ccntt from 1 to 100 by 1 do
ccntt:
Cbx:= coeff(bx,x^ccntt):
Cax:= coeff(ax,x^ccntt):
Ccx:= coeff(cx,x^(ccntt*2)):
a1 := a1 + Cax*x^ccntt:
a2 := a2 + Cax*x^(ccntt*2):
b1 := b1 + Cbx*x^ccntt:
b2 := b2 + Cbx*x^(ccntt*2):
b3 := b3 +Cbx*x^(ccntt*3):
c2 := c2 + Ccx*x^(ccntt*2):
c4 := c4 + Ccx*x^(ccntt*4):
c6 := c6 + Ccx*x^(ccntt*6):
end do:

"Achiral Alkanes + Enantiomeric Pairs";
UxAC := (x/24)*(b1^4 + 3*b2^2 + 8*b1*b3 + 6*a1^2*c2 + 6*c4)
- (1/4)*((b1-1)^2 + (b2-1) + (a1-1)^2 + (c2-1)):
BxAC := (1/2)*((b2-1) + (c2-1)):
NxAC := (x/24)*(b1^4 + 3*b2^2 + 8*b1*b3 + 6*a1^2*c2 + 6*c4)
- (1/4)*((b1-1)^2 - (b2-1) + (a1-1)^2 - (c2-1)):

"Print-Out of Results";
for ccntt from 1 to 100 by 1 do
printf("%d & %d & %d & %d \\\\ \n",
ccntt,
coeff(UxAC,x^ccntt),
coeff(BxAC,x^ccntt),
coeff(NxAC,x^ccntt));
end do;
```

In this code, the abbreviated symbols for functional equations are used as follows: `a1` for $a(x)$, `a2` for $a(x^2)$, `b1` for $b(x)$, and so on. The first paragraph ("Functional Equations for Alkyl Ligands") declares three functional equations (eqs. 11–13). In the 2nd paragraph ("Initial Values"), the initial values for the initial (trivial) planted 3D-tree are set to be $\alpha_0 = 1$, $\gamma_0 = 1$, and $\beta_0 = 1$ by encoding `a1 := 1; a2 := 1;` and so on. The 3rd paragraph ("Recursive

Calculation") involves a `do` loop for calculating $\alpha_k$, $\gamma_k$, and $\beta_k$ recursively ($1 \leq k \leq 100$) by using a Maple command `coeff`. After escaping from the `do` loop, the 4th paragraph ("Achiral Alkanes + Enantiomeric Pairs") declares the calculation of `UxAC` for $U(x)^{(AC)}$ (eq. 26), `BxAC` for $B(x)^{(AC)}$ (eq. 30), and `NxAC` for $N(x)^{(AC)}$ (eq. 33). The 5th paragraph (the final `do` loop named "Print-Out of Results") shows the print-out step of the calculation results.

The code is executed by inputting the following command on the Maple inputting window:

```
read "NUB-AC1-100.mpl";
```

Thereby, we obtain the coefficients $U_k^{(AC)}$ for eq. 24, $B_k^{(AC)}$ for eq. 28, and $N_k^{(AC)}$ for eq. 32, which are collected in Table 1.

# 5   Achiral and Chiral 3D-Trees

## 5.1   Itemization into Achiral and Chiral 3D-Trees

The methodology described for evaluating the total number of 3D-Trees (Fig. 4) is modified in order to itemize 3D-trees into achiral and chiral ones. The functional equation $\widehat{G}(x)^{(A)}$ for counting achiral uninuclear 3D-trees the functional equation $\widehat{G}(x)^{(C)}$ for counting chiral uninuclear 3D-trees exhibit irregular behaviors, which should be corrected to realize the achiral/chiral itemization, as shown in Fig. 7. The dichotomy between achiral balanced 3D-trees and achiral unbalanced ones as well as the dichotomy between chiral balanced 3D-trees and chiral unbalanced ones are useful guides to the itemized calculations.

## 5.2   Achiral 3D-Trees

### 5.2.1   Achiral Unbalanced 3D-Trees

To evaluate the gross number of achiral uninuclear 3D-trees, the first proposition of Theorem 4 for the enumeration of achiral ligands [20] is used to derive the following CI-CF$_A$:

$$\begin{aligned}
\text{CI-CF}_A(\mathbf{T}_d; a_d, b_d, c_d) &= 2\text{CI-CF}(\mathbf{T}_d; a_d, b_d, c_d) - \text{CI-CF}(\mathbf{T}; b_d) \\
&= \frac{1}{2}(a_1^2 c_2 + c_4),
\end{aligned} \tag{34}$$

which counts achiral promolecules only. By substituting $a(x^d)$, $c(x^d)$, and $b(x^d)$ for $a_d$, $c_d$, and $b_d$ in eq. 34, we obtain the following functional equation:

$$G(x)^{(A)} = \frac{x}{2}\{a(x)^2 c(x^2) + c(x^4)\}. \tag{35}$$

However, eq. 34 and the corresponding functional equation (eq. 35) underestimate *meso*-cases, which should be corrected as follows:

$$\frac{1}{2}(c_2 - a_2). \tag{36}$$

Note that the sphericity index $c_2$ evaluates a set of achiral ligands of the same kind along with a pair of enantiomeric ligands (i.e., a pseudoasymmetric case), while the sphericity index $a_2$ alternatively evaluates the set of achiral ligands of the same kind. Hence, the subtraction $\frac{1}{2}(c_2 -$

## Table 1: Numbers of 3D-Trees or Alkanes as Stereoisomers

| $k$ | $U_k^{(AC)}$ (Unbalanced 3D-trees) | $B_k^{(AC)}$ (Balanced 3D-trees) | $N_k^{(AC)}$ (Total 3D-trees) |
|---|---|---|---|
| 1 | 1 | 0 | 1 |
| 2 | 0 | 1 | 1 |
| 3 | 1 | 0 | 1 |
| 4 | 1 | 1 | 2 |
| 5 | 3 | 0 | 3 |
| 6 | 3 | 2 | 5 |
| 7 | 9 | 0 | 9 |
| 8 | 14 | 5 | 19 |
| 9 | 38 | 0 | 38 |
| 10 | 77 | 11 | 88 |
| 11 | 203 | 0 | 203 |
| 12 | 481 | 28 | 509 |
| 13 | 1299 | 0 | 1299 |
| 14 | 3385 | 74 | 3459 |
| 15 | 9347 | 0 | 9347 |
| 16 | 25691 | 199 | 25890 |
| 17 | 72505 | 0 | 72505 |
| 18 | 205326 | 551 | 205877 |
| 19 | 589612 | 0 | 589612 |
| 20 | 1702022 | 1553 | 1703575 |
| 21 | 4954686 | 0 | 4954686 |
| 22 | 14497672 | 4436 | 14502108 |
| 23 | 42671509 | 0 | 42671509 |
| 24 | 126167658 | 12832 | 126180490 |
| 25 | 374749447 | 0 | 374749447 |
| 26 | 1117468456 | 37496 | 1117505952 |
| 27 | 3344714436 | 0 | 3344714436 |
| 28 | 10045038039 | 110500 | 10045148539 |
| 29 | 30264120901 | 0 | 30264120901 |
| 30 | 91449349786 | 328092 | 91449677878 |
| 31 | 277096805630 | 0 | 277096805630 |
| 32 | 841782853026 | 980491 | 841783833517 |
| 33 | 2563418291362 | 0 | 2563418291362 |
| 34 | 7823943659908 | 2946889 | 7823946606797 |
| 35 | 23931052067297 | 0 | 23931052067297 |
| 36 | 73345824279219 | 8901891 | 73345833181110 |
| 37 | 225226025743122 | 0 | 225226025743122 |
| 38 | 692862443612081 | 27012286 | 692862470624367 |
| 39 | 2135109239262173 | 0 | 2135109239262173 |
| 40 | 6590223533710379 | 82300275 | 6590223616010654 |
| 41 | 20372876580255143 | 0 | 20372876580255143 |
| 42 | 63073132299024179 | 251670563 | 63073132550694742 |
| 43 | 195544793394348271 | 0 | 195544793394348271 |
| 44 | 607057683359184557 | 772160922 | 607057684131345479 |
| 45 | 1886989279103128211 | 0 | 1886989279103128211 |
| 46 | 5872733739773663554 | 2376294040 | 5872733742149957594 |
| 47 | 18298681742426380229 | 0 | 18298681742426380229 |
| 48 | 5708034047101942743 | 7333282754 | 5708034054435225497 |
| 49 | 178246302614039769705 | 0 | 178246302614039769705 |
| 50 | 557189473879833624598 | 22688455980 | 557189473902522080578 |
| 51 | 1743475977870305954708 | 0 | 1743475977870305954708 |
| 52 | 5460633705720107834856 | 70361242924 | 5460633705790469077780 |
| 53 | 17118606500538110493165 | 0 | 17118606500538110493165 |
| 54 | 53712728231114765739820 | 218679264772 | 53712728231333445004592 |
| 55 | 168676827177458246245600 | 0 | 168676827177458246245600 |
| 56 | 530139017193401578706086 | 681018679604 | 530139017194082597385690 |
| 57 | 1667507044106396700614662 | 0 | 1667507044106396700614662 |
| 58 | 5249007976438914262792265 | 2124842137550 | 5249007976441039104929815 |
| 59 | 16535111535321800418856805 | 0 | 16535111535321800418856805 |
| 60 | 52125067168086138719692353 | 6641338630714 | 52125067168092780058323067 |
| 61 | 164431691004690092819389801 | 0 | 164431691004690092819389801 |
| 62 | 5190558685480027791288810896 | 20792003301836 | 5190558685480048583292112732 |
| 63 | 1639544206288476255825253718 | 0 | 1639544206288476255825253718 |
| 64 | 5182076144231327740207559121 | 65193446172901 | 5182076144231392933653732022 |
| 65 | 16388819934893627771459167067 | 0 | 16388819934893627771459167067 |
| 66 | 51861705597581423492821877183 | 204709353135917 | 51861705597581628202175013100 |
| 67 | 164207682036849477130738064324 | 0 | 164207682036849477130738064324 |
| 68 | 520212032768970737917688722113 | 643665829838389 | 520212032768971381583518560502 |
| 69 | 1648923729893987703415359750119 | 0 | 1648923729893987703415359750119 |
| 70 | 5229345060893541830817748472471 | 2026461371823166 | 5229345060893543857279120295637 |
| 71 | 16592589875613236090913193392688 | 0 | 16592589875613236090913193392688 |
| 72 | 52673849989526617417137349471653 | 6387637263287353 | 52673849989526623804774612759006 |
| 73 | 167295424464204241785279087528744 | 0 | 167295424464204241785279087528744 |
| 74 | 531588444680524864888061177525111 | 20157546705808565 | 531588444680524885045607883333676 |
| 75 | 1689911835064564750230170718349855 | 0 | 1689911835064564750230170718349855 |
| 76 | 5374578409356516216313812375831610 | 63680191033811326 | 5374578409356516279994003409642936 |
| 77 | 17100609751074144217174560807768366 | 0 | 17100609751074144217174560807768366 |
| 78 | 54432817814305204592198172954475080 | 201379876145388644 | 54432817814305204793578049099863724 |
| 79 | 173335468778163767515568474781956550 | 0 | 173335468778163767515568474781956550 |
| 80 | 552188059690578419174290504433282587 | 637456295966779429 | 552188059690578419811746800400062016 |
| 81 | 17597673131496477955950136185436237113 | 0 | 17597673131496477955950136185436237113 |
| 82 | 561032495061053012413971272412341796 | 2019698989374464699 | 561032495061053014433670261786806495 |
| 83 | 178929249878033326824799846194126147310 | 0 | 178929249878033326824799846194126147310 |
| 84 | 5708623288721235607406086665154773147 | 6404799147037290651 | 5708623288721235671454078135527637798 |
| 85 | 182194157793655704794237473891139390912 | 0 | 182194157793655704794237473891139390912 |
| 86 | 58168378300498467718442584336692845727 | 20327740716521351562 | 58168378300498467921720325057824197289 |
| 87 | 1857742280338673467557442653721200301589 | 0 | 1857742280338673467557442653721200301589 |
| 88 | 593508092709183589738703184497798524048 | 64568510301289106574 | 593508092709183596306375966782406630622 |
| 89 | 18967377099179003868970637596678240906974 | 0 | 18967377099179003868970637596678240906974 |
| 90 | 60635122169340932631531262843012991399522 | 205250829465372138276 | 60635122169340932836782092465135537798 |
| 91 | 193898555422930447001151675263475562356 | 0 | 193898555422930447001151675263475562356 |
| 92 | 620233644123045351108744394299159832185642 | 652930625323502669516 | 620233644123046004039369722662502845158 |
| 93 | 1984557489015003230954102094778322440335524 | 0 | 1984557489015003230954102094778322440335524 |
| 94 | 6351801838823542109988548528197448226219 | 2078516705781154747150 | 6351801838825620626694330615951971369139 |
| 95 | 20335387509472990198674865937576370042014764 | 0 | 20335387509472990198674865937576370042014764 |
| 96 | 6512199033672232727910169348051542266045019 | 6621122347418605999236 | 6512199033672239349032516756657542265045019 |
| 97 | 208602785663318655583000176804691552968239008 | 0 | 208602785663318655583000176804691552968239008 |
| 98 | 6683860355753997432288498836647610817266908 | 21105194400328603264540 | 6683860355753997634403448 |
| 99 | 2142136450298921147961693542530974370563522319 | 0 | 2142136450298921147961693542530974370563522319 |
| 100 | 6867159545916447686442156397421880750323335689 | 673155671361795001083166 | 6867159545916447722371298901692982448185 |
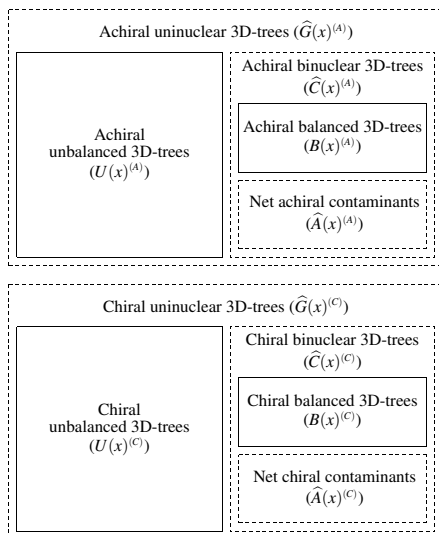
Figure 7: The dichotomy of balanced/unbalanced 3D-trees and for the dual recognition as un-inuclear 3D-trees and binuclear 3D-trees. The total number of achiral or chiral trees is obtained by summing up the number of unbalanced 3D-trees and the the number of 3D-balanced trees, i.e., $N(x)^{(A)} = U(x)^{(A)} + B(x)^{(A)}$ or $N(x)^{(C)} = U(x)^{(C)} + B(x)^{(C)}$.

$a_2$) leaves each pair of enantiomeric ligands, where the average by 1/2 is necessary because such a pair of enantiomeric ligands is doubly counted in terms of the enantiospheric character of $c_2$. This underestimation will be exemplified in the discussion of Fig. 8 later.

Let $\widehat{G}_k^{(A)}$ be the gross number of achiral uninuclear 3D-trees of carbon content $k$, which appears as each coefficient of the following generating function:

$$\widehat{G}(x)^{(A)} = \sum_{k=0}^{\infty} \widehat{G}_k^{(A)} x^k. \tag{37}$$

By substituting $a(x^d)$, $c(x^d)$, and $b(x^d)$ for $a_d$, $c_d$, and $b_d$ in eq. 34 as well as by substituting $a(x^d) - 1$ and $c(x^d) - 1$ for $a_d$ and $c_d$ in eq. 36, we obtain the following functional equation:

$$\widehat{G}(x)^{(A)} = \frac{x}{2} \{ a(x)^2 c(x^2) + c(x^4) \} + \frac{1}{2} \{ (c(x^2) - 1) - (a(x^2) - 1) \}, \tag{38}$$

in which the underestimation due to *meso*-cases has been corrected by adding the term shown in the second pair of braces. Note that, because eq. 34 for CI-CF$_A$($\mathbf{T}_d; a_d, b_d, c_d$) ignores the nucleus of the parent promolecule tentatively (cf. **8**), the term in the first pair of braces of the functional equation (eq. 38) is obtained by multiplying by $x$.

To evaluate achiral binuclear 3D-trees as contaminants, the first proposition of Theorem 4 for the enumeration of achiral ligands [20] is applied to this case so as to derive the following

CI-CF$_A$:

$$\text{CI-CF}_A(\mathbf{D}_{\infty h}; a_d, b_d, c_d) = 2\text{CI-CF}(\mathbf{D}_{\infty h}; a_d, b_d, c_d) - \text{CI-CF}(\mathbf{D}_{\infty}; b_d)$$
$$= \frac{1}{2}\left(a_1^2 + c_2\right), \tag{39}$$

which counts achiral uninuclear 3D-trees only.

Let $\widehat{C}_k^{(A)}$ be the number of achiral binuclear 3D-trees of carbon content $k$:

$$\widehat{C}(x)^{(A)} = \sum_{k=1}^{\infty} \widehat{C}_k^{(A)} x^k \tag{40}$$

By substituting $a(x^d) - 1$ and $c(x^d) - 1$ for $a_d$ and $c_d$ in eq. 39, we obtain the following functional equation:

$$\widehat{C}(x)^{(A)} = \frac{1}{2}\left\{(a(x) - 1)^2 + (c(x^2) - 1)\right\}. \tag{41}$$

Let $U_k^{(A)}$ be the number of achiral unbalanced 3D-trees of carbon content $k$, which appears as each coefficient of the following subtraction:

$$U(x)^{(A)} = \sum_{k=0}^{\infty} U_k^{(A)} x^k. \tag{42}$$

According to the relationship shown in Fig. 7, eq. 42 is evaluated by the following functional equation:

$$U(x)^{(A)} = \widehat{G}(x)^{(A)} - \widehat{C}(x)^{(A)}. \tag{43}$$

By introducing eq. 38 and eq. 41 into eq. 43, we obtain the following functional equation:

$$U(x)^{(A)} = \frac{x}{2}\left\{a(x)^2 c(x^2) + c(x^4)\right\} + \frac{1}{2}\left\{(c(x^2) - 1) - (a(x^2) - 1)\right\}$$
$$- \frac{1}{2}\left\{(a(x) - 1)^2 + (c(x^2) - 1)\right\}$$
$$= \frac{x}{2}\left\{a(x)^2 c(x^2) + c(x^4)\right\} - \frac{1}{2}\left\{(a(x) - 1)^2 + (a(x^2) - 1)\right\}. \tag{44}$$

The underestimation of *meso*-cases by eq. 34 or by the corresponding functional equation $G(x)^{(A)}$ (eq. 35) is exemplified by Fig. 8, where *meso*-3,4-dimethylhexane is depicted in terms of the dual recognition as uninuclear and binuclear 3D-trees. Note that the *meso*-3,4-dimethylhexane is an achiral balanced 3D-tree.

Although *meso*-3,4-dimethylhexane is achiral, the formulas (**24–29**) are recognized to be chiral uninuclear 3D-trees so that they do not contribute to $G(x)^{(A)}$ (eq. 35) nor to $\widehat{G}(x)^{(A)}$ (eq. 38). At the same time, the formulas (**24–29**) are recognized to be chiral binuclear 3D-trees so that they do not contribute to $\widehat{C}(x)^{(A)}$ (eq. 40). As the result, the cancellation mechanism shown in Fig. 7 works well in eq. 43, where even the incorrect determination of the achirality/chirality for **24–29** causes no erroneous effects.

In contrast, the formula (**23**) causes an irregular effect. The formula (**23**) is irregularly determined to be chiral if it is recognized as a uninuclear 3D-tree. This means that it does not contribute to the evaluation of achiral stereoisomers by $G(x)^{(A)}$ (eq. 35) so as to cause the underestimation of $G(x)^{(A)}$ (eq. 35) by one unit. Hence, the functional equation $G(x)^{(A)}$ should
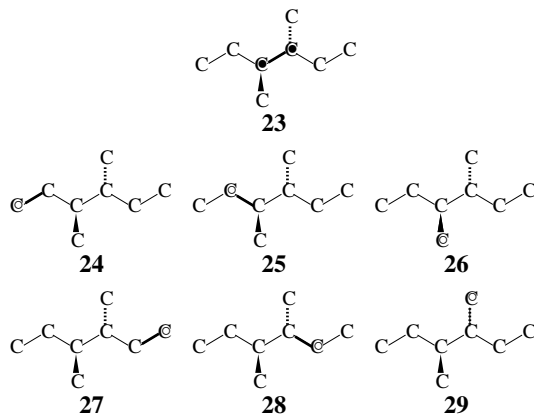
Figure 8: Balanced 3D-tree of *meso*-type. Cancellation between uninuclear 3D-trees and binuclear 3D-trees causes an irregular effect because the achirality/chirality of **23** is recognized irregularly.

be corrected to cover the underestimation by 1 due to each of such *meso*-cases as **23**, so that the correction of $G(x)^{(A)}$ (eq. 35) results in $\widehat{G}(x)^{(A)}$ (eq. 38).

If it is recognized as a binuclear tree, on the other hand, the formula (**23**) is determined to be achiral (i.e., as a pseudoasymmetric case). Hence, it contributes by 1 to $\widehat{C}(x)^{(A)}$ (eq. 40). It follows that the functional equation $U(x)^{(A)}$ (eq. 43) gives correct values of achiral unbalanced 3D-trees only when $\widehat{G}(x)^{(A)}$ is corrected as found in eq. 38.

### 5.2.2 Achiral Balanced 3D-Trees

Achiral balanced 3D-trees are symmetric binuclear 3D-trees represented by X—X ($\mathbf{D}_{\infty h}$) or p—$\overline{\mathrm{p}}$ ($\mathbf{C}_{\infty h}$), which are characterized by 2-cycles (i.e., $a_2$ and $c_2$). Although we here omit the details of the derivation, we obtain the following CI-CF:

$$\frac{1}{2}\left(a_2 + c_2\right),\tag{45}$$

where the top fraction (1/2) represents the average of the results due to the two terms at issue.

Let $B_k^{(A)}$ be the number of achiral balanced 3D-trees of carbon content $k$, which appears as the coefficient of $x^k$ in the following generating function:

$$B(x)^{(A)} = \sum_{k=1}^{\infty} B_k^{(A)} x^k.\tag{46}$$

By substituting $a(x^d) - 1$ and $c(x^d) - 1$ for $a_d$ and $c_d$ in the right-hand side of eq. 45, we obtain the corresponding functional equation:

$$B(x)^{(A)} = \frac{1}{2}\left\{(a(x^2) - 1) + (c(x^2) - 1)\right\}.\tag{47}$$

By combining eq. 41 with eq. 47, net contaminants are evaluated by the following functional equation:

$$\widehat{A}(x)^{(A)} = \widehat{C}(x)^{(A)} - B(x)^{(A)}$$
$$= \frac{1}{4}\{(a(x)-1)^2 - (a(x^2)-1)\}. \tag{48}$$

See Fig. 7 again to grasp this relationship.

### 5.2.3  Enumeration of Achiral 3D-Trees

Let $N_k^{(A)}$ be the total number of achiral 3D-trees of carbon content $k$, where the number of achiral 3D-trees and the number of enantiomeric pairs of chiral ones are summed up. The number $N_k^{(A)}$ is the coefficient of the term $x^k$ appearing in a generating function:

$$N(x)^{(A)} = \sum_{k=1}^{\infty} N_k^{(A)} x^k. \tag{49}$$

The generating function can be evaluated by summing up $U(x)^{(A)}$ and $B(x)^{(A)}$ or by subtracting $\widehat{A}(x)^{(A)}$ from $\widehat{G}(x)^{(A)}$. By summing up eq. 44 and eq. 47 or by subtracting eq. 48 from eq. 38, we obtain the following functional equation:

$$N(x)^{(A)} = \widehat{G}(x)^{(A)} - \widehat{A}(x)^{(A)}$$
$$= U(x)^{(A)} + B(x)^{(A)}$$
$$= \frac{x}{2}\{a(x)^2 c(x^2) + c(x^4)\} - \frac{1}{2}\{(a(x)-1)^2 - (c(x^2)-1)\}. \tag{50}$$

which gives the total number of achiral 3D-trees of carbon content $k$ as the coefficient of the term $x^k$.

### 5.2.4  Implementation of a Program for Counting Achiral 3D-Trees

The functional equations $U(x)^{(A)}$ (eq. 44), $B(x)^{(A)}$ (eq. 47), and $N(x)^{(A)}$ (eq. 50) are programmed by means of the Maple programming language to give the following code, which is stored in a file named "NUB-A1-100.mpl" tentatively.

A Maple program for counting achiral alkanes, "NUB-A1-100.mpl":

```
"Functional Equaitons for Alkyl Ligands";
(omitted)

"Initial Values";
(omitted)

"Recursive Calculation";
(omitted)

"Achiral Alkanes";
UxA := (x/2)*(a1^2*c2 + c4) - (1/2)*((a1-1)^2 + (a2-1)):
BxA := (1/2)*((a2-1) + (c2-1)):
NxA := (x/2)*(a1^2*c2 + c4) - (1/2)*((a1-1)^2 -(c2-1)):
```

Table 2: Numbers of Achiral 3D-Trees or Alkanes as Stereoisomers

| $k$ | $U_k^{(A)}$ (Achiral unbalanced 3D-trees) | $B_k^{(A)}$ (Achiral balanced 3D-trees) | $N_k^{(A)}$ (Total Achiral 3D-trees) |
|---|---|---|---|
| 1 | 1 | 0 | 1 |
| 2 | 0 | 1 | 1 |
| 3 | 1 | 0 | 1 |
| 4 | 1 | 1 | 2 |
| 5 | 3 | 0 | 3 |
| 6 | 3 | 2 | 5 |
| 7 | 7 | 0 | 7 |
| 8 | 10 | 4 | 14 |
| 9 | 21 | 0 | 21 |
| 10 | 32 | 8 | 40 |
| 11 | 61 | 0 | 61 |
| 12 | 100 | 18 | 118 |
| 13 | 186 | 0 | 186 |
| 14 | 311 | 44 | 355 |
| 15 | 567 | 0 | 567 |
| 16 | 970 | 111 | 1081 |
| 17 | 1755 | 0 | 1755 |
| 18 | 3029 | 296 | 3325 |
| 19 | 5454 | 0 | 5454 |
| 20 | 9495 | 811 | 10306 |
| 21 | 17070 | 0 | 17070 |
| 22 | 29857 | 2279 | 32136 |
| 23 | 53628 | 0 | 53628 |
| 24 | 94184 | 6520 | 100704 |
| 25 | 169175 | 0 | 169175 |
| 26 | 297941 | 18933 | 316874 |
| 27 | 535267 | 0 | 535267 |
| 28 | 944956 | 55568 | 1000524 |
| 29 | 1698322 | 0 | 1698322 |
| 30 | 3003887 | 164613 | 3168500 |
| 31 | 5400908 | 0 | 5400908 |
| 32 | 9568596 | 491227 | 10059823 |
| 33 | 17211368 | 0 | 17211368 |
| 34 | 30535539 | 1475197 | 32010730 |
| 35 | 54947147 | 0 | 54947147 |
| 36 | 97605577 | 4453995 | 102059572 |
| 37 | 175702378 | 0 | 175702378 |
| 38 | 312451188 | 13511597 | 325962785 |
| 39 | 562645937 | 0 | 562645937 |
| 40 | 1001535506 | 41159667 | 1042695173 |
| 41 | 1804088396 | 0 | 1804088396 |
| 42 | 3214198000 | 125852346 | 3340050346 |
| 43 | 5791497722 | 0 | 5791497722 |
| 44 | 10326520690 | 386110379 | 10712631069 |
| 45 | 18611821161 | 0 | 18611821161 |
| 46 | 33210027848 | 1188200648 | 34398228496 |
| 47 | 59870273288 | 0 | 59870273288 |
| 48 | 106901100844 | 3666735665 | 110567836509 |
| 49 | 192762694240 | 0 | 192762694240 |
| 50 | 344398254827 | 11344397151 | 355742651978 |
| 51 | 621145058010 | 0 | 621145058010 |
| 52 | 1110394575250 | 35180919588 | 1145575494838 |
| 53 | 2003060193783 | 0 | 2003060193783 |
| 54 | 3582665399751 | 109340167653 | 3692005567404 |
| 55 | 6464001746606 | 0 | 6464001746606 |
| 56 | 11567121483420 | 340510285076 | 11907631768496 |
| 57 | 20873421744449 | 0 | 20873421744449 |
| 58 | 37369250525887 | 1062422767060 | 38431673292947 |
| 59 | 67445191538640 | 0 | 67445191538640 |
| 60 | 120796806131358 | 3320672319811 | 124117478451169 |
| 61 | 218049903481679 | 0 | 218049903481679 |
| 62 | 390689856666232 | 10396007051826 | 401085903718058 |
| 63 | 705330165952872 | 0 | 705330165952872 |
| 64 | 1264240667134616 | 32596732656028 | 1296837399790644 |
| 65 | 2282686396696017 | 0 | 2282686396696017 |
| 66 | 4092934323957245 | 102354693779227 | 4195289017736472 |
| 67 | 7391016289967130 | 0 | 7391016289967130 |
| 68 | 13256686348542663 | 321832945456486 | 13578519293999149 |
| 69 | 23941657967808209 | 0 | 23941657967808209 |
| 70 | 42955539449512661 | 1013230740858730 | 43968770190371391 |
| 71 | 77586381466034947 | 0 | 77586381466034947 |
| 72 | 139244197528118594 | 3193818729252303 | 142438016257370897 |
| 73 | 251528935349306793 | 0 | 251528935349306793 |
| 74 | 451543239869815911 | 10078773528606385 | 461622013398422296 |
| 75 | 815741140338068227 | 0 | 815741140338068227 |
| 76 | 1464796231938726842 | 31840095829362305 | 1496636327768089147 |
| 77 | 2646489896299591485 | 0 | 2646489896299591485 |
| 78 | 4753381883431698309 | 100689938635340259 | 4854071822067038568 |
| 79 | 8588824555686539622 | 0 | 8588824555686539622 |
| 80 | 15430088486653345592 | 318728148984934750 | 15748816637638284342 |
| 81 | 27882748457230290862 | 0 | 27882748457230290862 |
| 82 | 50103432788380077848 | 1009849496491319969 | 51113282284871397817 |
| 83 | 90545956172141260398 | 0 | 90545956172141260398 |
| 84 | 162739708060789718347 | 3202399576732860390 | 165942107637522578737 |
| 85 | 294122275423916054352 | 0 | 294122275423916054352 |
| 86 | 528738145185319822974 | 10163870364052173503 | 538902015549317996477 |
| 87 | 955666449267540395221 | 0 | 955666449267540395221 |
| 88 | 1718317030140838398434 | 32284255160971103895 | 1750601285301809502329 |
| 89 | 3105981799108470323147 | 0 | 3105981799108470323147 |
| 90 | 5585683651585644442875 | 102625414751297888081 | 5688309066336942330956 |
| 91 | 10097190706324159336800 | 0 | 10097190706324159336800 |
| 92 | 18161635403115174163032 | 326465312694961416234 | 18488100715810135579266 |
| 93 | 32832697580700874763572 | 0 | 32832697580700874763572 |
| 94 | 59065602840222573478256 | 1039258352950447646863 | 60104861193173021125119 |
| 95 | 106785552739916704811839 | 0 | 106785552739916704811839 |
| 96 | 192137075503251426124774 | 3310561173816204194750 | 195447636677067630319524 |
| 97 | 347387515383940750498193 | 0 | 347387515383940750498193 |
| 98 | 625144758967206852442222 | 10552597200357064320094 | 635697356167563916762316 |
| 99 | 1130336590391716286395368 | 0 | 1130336590391716286395368 |
| 100 | 2034413226413485412716350 | 335677835684344148965571 | 2068070109981919561681921 |

```
for ccntt from 1 to 100 by 1 do
printf("%d & %d & %d & %d \\\\ \n",
ccntt,
coeff(UxA,x^ccntt),
coeff(BxA,x^ccntt),
coeff(NxA,x^ccntt));
end do;
```

In this code, the three paragraphs for "Functional Equations for Alkyl Ligands", "Initial Values", and "Recursive Calculation" are omitted because they are the same as those the code described above ("NUB-AC1-100.mpl"). The 4th paragraph ("Achiral Alkanes") declares the calculation of $UxA$ for $U(x)^{(A)}$ (eq. 44), $BxA$ for $B(x)^{(A)}$ (eq. 47), and $NxA$ for $N(x)^{(A)}$ (eq. 50). The 5th paragraph (the final do loop named "Print-Out of Results") shows the print-out of the calculation results.

The code is executed by inputting from the Maple inputting window. Thereby, we obtain the coefficients $U_k^{(A)}$ for eq. 42, $B_k^{(A)}$ for eq. 46, and $N_k^{(A)}$ for eq. 49, which are collected in Table 2 up to carbon content 100.

## 5.3 Chiral 3D-Trees

### 5.3.1 Chiral Unbalanced 3D-Trees

To evaluate the gross number of chiral 3D-trees, the second proposition of Theorem 4 for the enumeration of chiral ligands [20] is used to obtain the following CI-CF$_C$:

$$\begin{aligned}
\text{CI-CF}_C(\mathbf{T}_d; a_d, b_d, c_d) &= \text{CI-CF}(\mathbf{T}, b_d) - \text{CI-CF}(\mathbf{T}_d, a_d, b_d, c_d) \\
&= \frac{1}{24}(b_1^4 + 3b_2^2 + 8b_1b_3 - 6a_1^2c_2 - 6c_4),
\end{aligned} \tag{51}$$

which counts chiral promolecules only, where each pair of enantiomers is counted just once. By substituting $a(x^d)$, $c(x^d)$, and $b(x^d)$ for $a_d$, $c_d$, and $b_d$ in eq. 51, we can obtain the following functional equation:

$$G(x)^{(C)} = \frac{x}{24}\{b(x)^4 + 3b(x^2)^2 + 8b(x)b(x^3) - 6a(x)^2c(x^2) - 6c(x^4)\}. \tag{52}$$

In contrast to eqs. 34 and 35, eq. 51 and the corresponding functional equation $G(x)^{(C)}$ (eq. 52) overestimate *meso*-cases, which should be reversely corrected by means of eq. 36. Remember **23** (Fig. 8), which reversely causes the overestimation of $G(x)^{(C)}$.

Let $\widehat{G}_k^{(C)}$ be the gross number of chiral uninuclear 3D-trees, where each pair of two enantiomers is counted just once. The corresponding generating function for enumerating them is represented as follows:

$$\widehat{G}(x)^{(C)} = \sum_{k=0}^{n} \widehat{G}_k^{(C)} x^k. \tag{53}$$

By substituting $a(x^d)-1$, $c(x^d)-1$, and $b(x^d)-1$ for $a_d$, $c_d$, and $b_d$ in 36 and by substituting $a(x^d)$, $c(x^d)$, and $b(x^d)$ for $a_d$, $c_d$, and $b_d$ in eq. 51, we can obtain the following functional equation:

$$\begin{aligned}
\widehat{G}(x)^{(C)} &= \frac{x}{24}\{b(x)^4 + 3b(x^2)^2 + 8b(x)b(x^3) - 6a(x)^2c(x^2) - 6c(x^4)\} \\
&\quad - \frac{1}{2}\{(c(x^2)-1) - (a(x^2)-1)\}. \tag{54}
\end{aligned}$$

To estimate chiral binuclear 3D-trees, the second proposition of Theorem 4 for the enumeration of chiral ligands [20] can be applied to obtain the following CI-CF$_C$:

$$
\begin{aligned}
\text{CI-CF}_C(\mathbf{D}_{\infty h}; a_d, b_d, c_d) &= \text{CI-CF}(\mathbf{D}_{\infty}; b_d) - \text{CI-CF}(\mathbf{D}_{\infty h}; a_d, b_d, c_d) \\
&= \frac{1}{4}\left(b_1^2 + b_2 - a_1^2 - c_2\right),
\end{aligned}
\tag{55}
$$

which counts chiral promolecules only.

Let $\widehat{C}_k^{(C)}$ be the number of binuclear 3D-trees of carbon content $k$, which are enantiomeric pairs of chiral ones:

$$
\widehat{C}(x)^{(C)} = \sum_{k=1}^{\infty} \widehat{C}_k^{(C)} x^k.
\tag{56}
$$

By replacing $a_d$, $c_d$, and $b_d$ by $a(x^d) - 1$, $c(x^d) - 1$, and $b(x^d) - 1$ respectively, eq. 55 is converted into the corresponding functional equation as follows:

$$
\widehat{C}(x)^{(C)} = \frac{1}{4}\left\{(b(x) - 1)^2 + (b(x^2) - 1) - (a(x) - 1)^2 - (c(x^2) - 1)\right\}.
\tag{57}
$$

Let $U_k^{(C)}$ be the number of chiral unbalanced 3D-trees, where each pair of two enantiomers is counted just once. The corresponding generating function for enumerating them is represented as follows:

$$
U(x)^{(C)} = \sum_{k=0}^{n} U_k^{(C)} x^k.
\tag{58}
$$

According to the methodology shown in Fig. 7, the subtraction of eq. 57 from eq. 54 gives the following functional equation:

$$
\begin{aligned}
U(x)^{(C)} &= \widehat{G}(x)^{(C)} - \widehat{C}(x)^{(C)} \\
&= \frac{x}{24}\left(b(x)^4 + 3b(x^2)^2 + 8b(x)b(x^3) - 6a(x)^2 c(x^2) - 6c(x^4)\right) \\
&\quad - \frac{1}{2}\left\{(c(x^2) - 1) - (a(x^2) - 1)\right\} \\
&\quad - \frac{1}{4}\left\{(b(x) - 1)^2 + (b(x^2) - 1) - (a(x) - 1)^2 - (c(x^2) - 1)\right\}. \\
&= \frac{x}{24}\left(b(x)^4 + 3b(x^2)^2 + 8b(x)b(x^3) - 6a(x)^2 c(x^2) - 6c(x^4)\right) \\
&\quad - \frac{1}{4}\left\{(b(x) - 1)^2 + (b(x^2) - 1) - (a(x) - 1)^2 + (c(x^2) - 1) - 2(a(x^2) - 1)\right\}. \quad (59)
\end{aligned}
$$

### 5.3.2 Chiral Balanced 3D-Trees

Chiral balanced 3D-trees are asymmetric binuclear trees represented by p—p/p̄—p̄ ($\mathbf{D}_{\infty}$), which are characterized by 2-cycles (i.e., $b_2$ minus $a_2$). Although we here omit the details of the derivation, we obtain the following CI-CF:

$$
\frac{1}{2}\left(b_2 - a_2\right),
\tag{60}
$$

where the top fraction (1/2) represents the average of the results due to the two terms at issue.

Let $B_k^{(C)}$ be the number of achiral balanced 3D-trees of carbon content $k$, which appears as the coefficient of $x^k$ in the following generating function:

$$B(x)^{(C)} = \sum_{k=1}^{\infty} B_k^{(C)} x^k. \tag{61}$$

By substituting $a(x^d) - 1$ and $b(x^d) - 1$ for $a_d$ and $b_d$ in the right-hand side of eq. 61, we obtain the corresponding functional equation:

$$B(x)^{(C)} = \frac{1}{2} \left\{ (b(x^2) - 1) - (a(x^2) - 1) \right\}. \tag{62}$$

By combining eq. 57 with eq. 62, net contaminants are evaluated by the following functional equation:

$$\begin{aligned}
\widehat{A}(x)^{(C)} &= \widehat{C}(x)^{(C)} - B(x)^{(C)} \\
&= \frac{1}{4} \left\{ (b(x) - 1)^2 - (b(x^2) - 1) - (a(x) - 1)^2 - (c(x^2) - 1) + 2(a(x^2) - 1) \right\}. \tag{63}
\end{aligned}$$

In order to grasp this relationship, refer to the bottom part of Fig. 7.

### 5.3.3 Enumeration of Chiral 3D-Trees

Let $N_k^{(C)}$ be the total number of chiral 3D-trees of carbon content $k$, where each enantiomeric pair of chiral 3D-trees is counted just once. The number $N_k^{(C)}$ is the coefficient of the term $x^k$ appearing in a generating function:

$$N(x)^{(C)} = \sum_{k=1}^{\infty} N_k^{(C)} x^k. \tag{64}$$

The generating function is evaluated by summing up $U(x)^{(C)}$ (eq. 59) and $B(x)^{(C)}$ (eq. 62) or by subtracting $\widehat{A}(x)^{(C)}$ (eq. 63) from $\widehat{G}(x)^{(C)}$ (eq. 54). Thereby, we obtain the following functional equation:

$$\begin{aligned}
N(x)^{(C)} &= \widehat{G}(x)^{(C)} - \widehat{A}(x)^{(C)} \\
&= U(x)^{(C)} + B(x)^{(C)} \\
&= \frac{x}{24} \left( b(x)^4 + 3b(x^2)^2 + 8b(x)b(x^3) - 6a(x)^2 c(x^2) - 6c(x^4) \right) \\
&\quad - \frac{1}{4} \left\{ (b(x) - 1)^2 - (b(x^2) - 1) - (a(x) - 1)^2 + (c(x^2) - 1) \right\}. \tag{65}
\end{aligned}$$

which gives the total number of chiral 3D-trees of carbon content $k$ as the coefficient of the term $x^k$.

### 5.3.4 Implementation of a Program for Counting Chiral 3D-Trees

The functional equations $U(x)^{(C)}$ (eq. 59), $B(x)^{(C)}$ (eq. 62), and $N(x)^{(C)}$ (eq. 65) are programmed by means of the Maple programming language. The resulting code is stored in a file named "NUB-C1-100.mpl" tentatively as follows.

A Maple program for counting chiral alkanes, "NUB-C1-100.mpl":

Table 3: Numbers of Chiral 3D-Trees or Alkanes as Stereoisomers

| $k$ | $U_k^{(C)}$ (Chiral unbalanced 3D-trees) | $B_k^{(C)}$ (Chiral balanced 3D-trees) | $N_k^{(C)}$ (Total Chiral 3D-trees) |
|---|---|---|---|
| 1 | 0 | 0 | 0 |
| 2 | 0 | 0 | 0 |
| 3 | 0 | 0 | 0 |
| 4 | 0 | 0 | 0 |
| 5 | 0 | 0 | 0 |
| 6 | 0 | 0 | 0 |
| 7 | 2 | 0 | 2 |
| 8 | 4 | 1 | 5 |
| 9 | 17 | 0 | 17 |
| 10 | 45 | 3 | 48 |
| 11 | 142 | 0 | 142 |
| 12 | 381 | 10 | 391 |
| 13 | 1113 | 0 | 1113 |
| 14 | 3074 | 30 | 3104 |
| 15 | 8780 | 0 | 8780 |
| 16 | 24721 | 88 | 24809 |
| 17 | 70750 | 0 | 70750 |
| 18 | 202297 | 255 | 202552 |
| 19 | 584158 | 0 | 584158 |
| 20 | 1692527 | 742 | 1693269 |
| 21 | 4937616 | 0 | 4937616 |
| 22 | 14467815 | 2157 | 14469972 |
| 23 | 42617881 | 0 | 42617881 |
| 24 | 126073474 | 6312 | 126079786 |
| 25 | 374580272 | 0 | 374580272 |
| 26 | 1117170515 | 18563 | 1117189078 |
| 27 | 3344179169 | 0 | 3344179169 |
| 28 | 10044093083 | 54932 | 10044148015 |
| 29 | 30262422579 | 0 | 30262422579 |
| 30 | 91446345899 | 163479 | 91446509378 |
| 31 | 277091404722 | 0 | 277091404722 |
| 32 | 841773284430 | 489264 | 841773773694 |
| 33 | 2563401079994 | 0 | 2563401079994 |
| 34 | 7823910181480 | 1471692 | 7823911653172 |
| 35 | 23930997120150 | 0 | 23930997120150 |
| 36 | 73345726673642 | 4447896 | 73345731121538 |
| 37 | 225225850040744 | 0 | 225225850040744 |
| 38 | 692862131160893 | 13500689 | 692862144661582 |
| 39 | 2135108676616236 | 0 | 2135108676616236 |
| 40 | 6590222532174873 | 41140608 | 6590222573315481 |
| 41 | 20372874776166747 | 0 | 20372874776166747 |
| 42 | 63073129084826179 | 125818217 | 63073129210644396 |
| 43 | 195544787602887105 | 0 | 195544787602887105 |
| 44 | 607057673032663867 | 386050543 | 607057673418714410 |
| 45 | 1886989260491307050 | 0 | 1886989260491307050 |
| 46 | 5872733706563635706 | 1188093392 | 5872733707751729098 |
| 47 | 18298681682556106941 | 0 | 18298681682556106941 |
| 48 | 57080340430000841899 | 3666547089 | 57080340433667388988 |
| 49 | 178246302421277075465 | 0 | 178246302421277075465 |
| 50 | 557189473535435369771 | 11344058829 | 557189473546779428600 |
| 51 | 1743475977249160896698 | 0 | 1743475977249160896698 |
| 52 | 5460633704609713259606 | 35180323336 | 5460633704644893582942 |
| 53 | 17118606498535050299382 | 0 | 17118606498535050299382 |
| 54 | 53712728227532100340069 | 109339097119 | 53712728227641439437188 |
| 55 | 168676827170994244498994 | 0 | 168676827170994244498994 |
| 56 | 530139017181834457722666 | 340508394528 | 530139017182174966117194 |
| 57 | 1667507044085523278870213 | 0 | 1667507044085523278870213 |
| 58 | 5249007976401545012266378 | 1062419370490 | 5249007976402607431636868 |
| 59 | 16535111535254355227318165 | 0 | 16535111535254355227318165 |
| 60 | 52125067167965341913560995 | 3320666310903 | 52125067167968662579871898 |
| 61 | 164431691004472878290416331 | 0 | 164431691004472878290416331 |
| 62 | 519055868547637101402144664 | 10395996250010 | 519055868547647398394674 |
| 63 | 1639544206288057228087300846 | 0 | 1639544206288057228087300846 |
| 64 | 5182076144230063499540424505 | 32596713516873 | 5182076144230096096253941378 |
| 65 | 16388819934891345085062471050 | 0 | 16388819934891345085062471050 |
| 66 | 51861705597577330558497919938 | 1023546593566900 | 51861705597574329131572766628 |
| 67 | 164207682036842086114448097194 | 0 | 164207682036842086114448097194 |
| 68 | 520212032768957481231340179450 | 321832884381903 | 520212032768957803064224561353 |
| 69 | 1648923729893963761757391941910 | 0 | 1648923729893963761757391941910 |
| 70 | 5229345060893498875278298959810 | 1013203063096436 | 5229345060893499888508929924246 |
| 71 | 16592589875613158504531727235741 | 0 | 16592589875613158504531727235741 |
| 72 | 52673849989526478172939821353059 | 319381853403506 | 52673849989526481366758355388109 |
| 73 | 167295424464203990256343738221951 | 0 | 167295424464203990256343738221951 |
| 74 | 531588444680524413344821307709200 | 10078773177202180 | 531588444680524423423594849113380 |
| 75 | 1689911835064563934890303802681628 | 0 | 1689911835064563934890303802681628 |
| 76 | 5374578409336514748341950437104768 | 31840095204449021 | 5374578409356514780120456415533789 |
| 77 | 17100609751074141570684664508176881 | 0 | 17100609751074141570684664508176881 |
| 78 | 544328178143051998388162895227676771 | 10068993751004838 5 | 544328178143051999395062270328253186 |
| 79 | 173335468778163758926743919095416928 | 0 | 173335468778163758926743919095416928 |
| 80 | 552188059695078403744202015784936995 | 318728146981844679 | 552188059695078404062930162766781674 |
| 81 | 1759767313496477928067387728205946251 | 0 | 1759767313496477928067387728205946251 |
| 82 | 5610324950610530074036279935743339948 | 10098494928883144730 | 5610324950610530075046129428626484678 |
| 83 | 17892924987803326734253890021984886912 | 0 | 17892924987803326734253890021984886912 |
| 84 | 57086232887213560571464159307630339772 | 32023995703044430261 | 57086232887213560574666558870794770033 |
| 85 | 182194157793655704500115198467223336560 | 0 | 182194157793655704500115198467223336560 |
| 86 | 581683783004984676655687698181609022753 | 10163870352469178059 | 581683783004984676665851568534078200812 |
| 87 | 1857742280338673466601776204453659906368 | 0 | 1857742280338673466601776204453659906368 |
| 88 | 5935080927091835895668714814836960125614 | 32284255140318002679 | 5935080927091835895700999069977278128293 |
| 89 | 18967377099179003865864655797569778746527 | 0 | 18967377099179003865864655797569778746527 |
| 90 | 60635122169340932625945579191427344966647 | 10262554147140742501 95 | 60635122169340932626340482046061441421896842 |
| 91 | 193898555422930446991054484557154282219435 | 0 | 193898555422930446991054484557154282219435 |
| 92 | 620233644123045351090582758896044658022610 | 32646531262854125328 2 | 620233644123045351090909224208673199275892 |
| 93 | 1984557489015003230921266939719762156559235 | 0 | 1984557489015003230921266939719762156559235 |
| 94 | 6351801838823542109929519249979522249143733 | 1039258352830707100287 | 6351801838823542109930558508332352956244020 |
| 95 | 20335387509472990198568083848364533372032925 | 0 | 20335387509472990198568083848364533372032925 |
| 96 | 65121990336372237275988798593019427521009 | 3310561173602401804486 | 65121990336372237276021904204755051963525495 |
| 97 | 208602785663318655582652789289307612217740815 | 0 | 208602785663318655582652789289307612217740815 |
| 98 | 668386035573399743228217843607508901320126 | 10552597199971538944446 | 668386035573399743228236204078120857245071132 |
| 99 | 2142136450298921147960563205940582654277126951 | 0 | 2142136450298921147960563205940582654277126951 |
| 100 | 6867159545916447686440121984195467264910619339 | 3365778356774535211 7595 | 6867159545916447686440155641979035010262736934 |

```
"Functional Equaitons for Alkyl Ligands";
(omitted)

"Initial Values";
(omitted)

"Recursive Calculation";
(omitted)

"Chiral Alkanes";
UxC := (x/24)*(b1^4 + 3*b2^2 + 8*b1*b3 - 6*a1^2*c2 - 6*c4)
- (1/4)*((b1-1)^2 + (b2-1) - (a1-1)^2 + (c2-1) - 2*(a2-1)):
BxC := (1/2)*((b2-1) - (a2-1)):
NxC := (x/24)*(b1^4 + 3*b2^2 + 8*b1*b3 - 6*a1^2*c2 - 6*c4)
- (1/4)*((b1-1)^2 - (b2-1) - (a1-1)^2 + (c2-1)):

for ccntt from 1 to 100 by 1 do
printf("%d & %d & %d & %d \\\\ \n",
ccntt,
coeff(UxC,x^ccntt),
coeff(BxC,x^ccntt),
coeff(NxC,x^ccntt));
end do;
```

Because the three paragraphs for "Functional Equations for Alkyl Ligands", "Initial Values", and "Recursive Calculation" are the same as described above ("NUB-AC1-100.mpl"), they are omitted. The 4th paragraph ("Chiral Alkanes") declares the calculation of UxC for $U(x)^{(C)}$ (eq. 59), BxC for $B(x)^{(C)}$ (eq. 62), and NxC for $N(x)^{(C)}$ (eq. 65). The 5th paragraph (the final do loop named "Print-Out of Results") shows the print-out step of the calculation results.

The code is executed on the Maple inputting window. Thereby, we obtain the coefficients $U_k^{(A)}$ for eq. 58, $B_k^{(A)}$ for eq. 61, and $N_k^{(A)}$ for eq. 64. They are collected in Table 3 up to carbon content 100.

# 6 Discussions

## 6.1 Cores vs. Twin-Cores

In connection with Fig. 4, the dichotomy between balanced and unbalanced 3D-trees is understandable in terms of the distinct effects of cores vs. twin-cores, as summarized in Table 4. It should be emphasized that a twin-core corresponds to a balance-edge (cf. Fig. 5), while a core corresponds to no edges (cf. Fig. 6).

1. Each of balanced 3D-trees is characterized by a balance-edge, which is contained in a representative binuclear 3D-tree (cf. Fig. 5). From a viewpoint of vertices, each balanced 3D-tree, which is to be counted just once, has a twin-core and the remaining uninuclei. From a view point of edges, each balanced 3D-tree has slant-edges and a balanced edge.

   The two viewpoints are correlated to each other by means of the correspondence between the slant-edges and the uninuclei (except the twin-core). This correspondence causes the cancellation between uninuclear 3D-trees and binuclear 3D-trees in the evaluation of balanced 3D-trees (cf. Fig. 5). Moreover, the twin-core corresponds to the balance-edge in one-to-one fashion so that the uninuclear 3D-tree (for the twin-core) and the

Table 4: Vertices and Edges in Balanced and Unbalanced 3D-Trees

| dichotomy | vertices | | | | edges | | |
|---|---|---|---|---|---|---|---|
| balanced 3D-trees | a twin-core | + | uninuclei | $\leftrightarrow$ | slant-edges | + | a balance-edge |
| unbalanced 3D-trees | a core | + | uninuclei | $\leftrightarrow$ | slant-edges | | (none) |
| | uninuclear 3D-Trees | | | | binuclear 3D-trees | | |

binuclear 3D-tree (for the balance-edge) cancel out each other (cf. Fig. 5). It follows that $G(x)^{(AC)} - C(x)^{(AC)}$ leaves no balanced 3D-trees, as shown in Fig. 4.

2. Each of unbalanced 3D-trees is characterized by a core, which is contained in a representative uninuclear 3D-tree selected from a set of uninuclear 3D-trees (cf. Fig. 6). From a viewpoint of vertices, each unbalanced 3D-tree, which is to be counted just once, has a core and the remaining uninuclei. Thereby, each unbalanced 3D-tree can be regarded as as a kind of rooted or planted 3D-tree, if its core is regarded as a root or as a principal vertex incident to a root. From a view point of edges, each unbalanced 3D-tree has slant-edges and no balanced edges.

The two viewpoints are correlated to each other by means of the correspondence between the slant-edges and the uninuclei (except the core). This correspondence causes the cancellation between uninuclear 3D-trees and binuclear 3D-trees in the evaluation of unbalanced 3D-trees (cf. Fig. 5). However, the core does not corresponds to any edge so that the uninuclear 3D-tree (for the core) is retained to be counted as an unbalanced 3D-tree (cf. Fig. 6). It follows that $G(x)^{(AC)} - C(x)^{(AC)}$ leaves unbalanced 3D-trees to be counted, as shown in Fig. 4.

## 6.2 Chirality and Achirality During Cancellation

An edge other than a balance-edge is called a slant-edge whether it is contained in balanced or unbalanced 3D-trees. Binuclear 3D-trees based on a slant-edge are categorized into four types shown in Fig. 9, if we take account of the superiority of the terminal vertices.
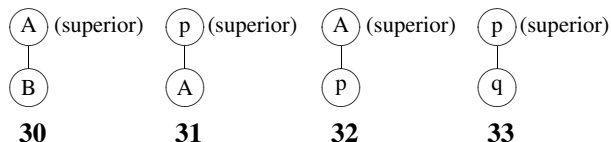


Figure 9: Binuclear 3D-trees based on a slant-edge. The symbols A and B represent achiral proligands, while p and q represent chiral proligands.

The chirality/achirality of a binuclear 3D-tree based on a slant-edge is identical with the chirality/achirality of the corresponding uninuclear 3D-trees.

1. Suppose that a binuclear 3D-tree based on a slant-edge is regarded as being chiral. Then, it is represented by either of the formulas **31**–**33**. Let us consider the terminal vertex other than the superior vertex of each formula as a uninucleus for generating uninuclear 3D-trees. If the resulting 3D-trees are achiral, the A of A–p should be chiral ($\overline{p}$ for a *meso*-case), the p of p–A should be achiral, and the q of q–p should $\overline{p}$ for a *meso*-case. These conclusions are inconsistent with the original presumption. Hence, the resulting uninuclear 3D-trees are concluded to be chiral.

2. Suppose that a binuclear tree based on a slant-edge is regarded as being achiral. Then, it is represented by the formula **30**. Let us consider the terminal vertex other than the superior vertex of each formula as a uninucleus for generating uninuclear 3D-trees. The resulting uninuclear 3D-trees are concluded to be achiral.

Binuclear 3D-trees based on a balance-edge are categorized into three types shown in Fig. 10. The irregular assignments pointed out in Fig. 7 are ascribed to *meso*-compounds of type p—$\overline{p}$.
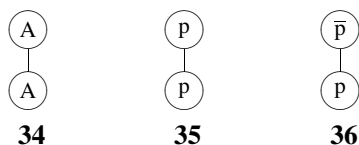


Figure 10: Binuclear 3D-trees based on a balance-edge. The symbol A represents an achiral proligand which p and $\overline{p}$ represent a enantiomeric pair of chiral proligands.

1. An achiral binuclear 3D-tree of type A—A (**34**) can be regarded as a uninuclear 3D-tree if the upper A is fixed and the lower A contains a uninucleus to be taken into consideration. So long as the lower A covers achiral proligands, the resulting uninuclear 3D-trees are achiral. Note that the two A's are not equalized under the action of $\mathbf{T}_d$ generating the uninuclear 3D-trees.

2. A chiral binuclear 3D-tree of type p—p/$\overline{p}$—$\overline{p}$ (**35**) can be regarded as a uninuclear 3D-tree if the upper p (or $\overline{p}$) is fixed and the lower p (or $\overline{p}$) contains a uninucleus to be taken into consideration. So long as the lower p covers chiral proligands, the resulting uninuclear 3D-trees are chiral. Note that the two p's (or $\overline{p}$'s) are not equalized under the action of $\mathbf{T}_d$ generating the uninuclear 3D-trees.

3. With respect to achiral binuclear trees of type p—$\overline{p}$ (**36**), we have discussed in terms of *meso*-cases in Fig. 8. The discussion for Fig. 8 can be extended to cover general cases. Although the p and the $\overline{p}$ are equalized under the action of $\mathbf{D}_{\infty h}$ for binuclear 3D-trees, they are not equalized under the action of $\mathbf{T}_d$ for the corresponding uninuclear 3D-tree. This means that the uninuclear 3D-tree is recognized to be chiral under the action of $\mathbf{T}_d$.

Consequently, the *meso*-cases (**36**) cause the underestimation of $\widehat{G}(x)^{(A)}$ (eq. 38) and the relevant overestimation of $\widehat{G}(x)^{(C)}$ (eq. 51).

## 6.3    Illustrative Examples of Balanced 3D-Trees

Because a chiral balanced 3D-tree of the type p—p (or $\bar{p}$—$\bar{p}$) corresponds to an achiral balanced 3D-tree of the special type p—$\bar{p}$ (i.e., a *meso*-compound), the existence of the former one assures the occurrence of the latter one. By examining the $B_k^{(C)}$-column of Table 3, the non-zero values of $B_k^{(C)}$ (for $k \geq 8$) indicate that the number $B_k^{(C)}$ of the corresponding *meso*-compounds are involved in the number $B_k^{(A)}$ of achiral balanced 3D-trees.

In order to exemplify the discussion in the preceding paragraph, let us examine balanced 3D-trees (alkanes) of carbon content 10. There exist eleven balanced 3D-trees, as found by the value $B_{10}^{(AC)} = 11$ (Table 1), which is partitioned into $B_{10}^{(A)} = 8$ for achiral stereoisomers (Table 2) and $B_{10}^{(C)} = 3$ for chiral stereoisomers (Table 3). The eight achiral balanced 3D-trees of carbon content 10 are depicted in Fig. 11, while the three chiral balanced 3D-trees of carbon content 10 are depicted in Fig. 12.
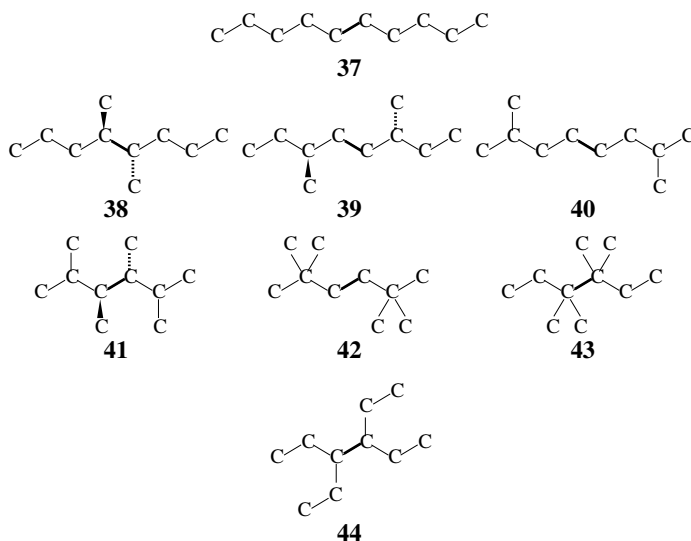


Figure 11: Achiral balanced alkanes (3D-trees) of carbon content 10. Among them, **38**, **39**, and **41** are *meso*-compounds. A boldfaced edge is a balance-edge.

Among the eight achiral balanced 3D-trees depicted in Fig. 11, three achiral 3D-trees, i.e., **38**, **39**, and **41**, are *meso*-compounds (p—$\bar{p}$). They respectively correspond to three chiral 3D-trees (p—p), i.e., **45**, **46**, and **47**, as depicted in Fig. 12. Note that p—p ($\bar{p}$—$\bar{p}$) and p—$\bar{p}$ are identical as graphs, where the pair p—p and p—$\bar{p}$ represents a single constitutional isomer, e.g., a pair of **38** and **45**, a pair of **39** and **46**, and a pair of **41** and **47**.

## 6.4    Comments on an Earlier Accomplishment

Several comments on an earlier report by Robinson et al. [27] should be added in order to emphasize the effect of the sphericity concept. If we follows the present notations, their equation
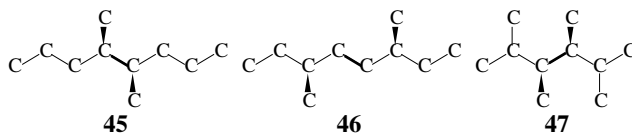
Figure 12: Chiral balanced alkanes (3D-trees) of carbon content 10. Either one is depicted as a representative of each pair of enantiomeric alkanes. A boldfaced edge is a balance-edge.

for evaluating the number of achiral isomers (eq. 19 of [27]) is represented by the following equation:

$$T(x)^{(A)} = \frac{x}{2}\{a(x)^2 s(x^2) + s(x^4)\},\tag{66}$$

where the variables $s(x^2)$ and $s(x^4)$ without sphericity were used in place of the present component functions $c(x^2)$ and $c(x^4)$, which are used in eq. 35 on the basis of the corresponding SIs ($c_2$ and $c_4$). The disregard of the sphericity in their treatment implies that the following ligand inventories were used:

$$a(x^d) = A^d + B^d + X^d + Y^d \tag{67}$$

$$s(x^d) = A^d + B^d + X^d + Y^d + p^d + \bar{p}^d,\tag{68}$$

if achiral alkyl ligands are represented by the symbols A, B, X, Y; and an enantiomeric pair of chiral alkyl ligands is represented by p and $\bar{p}$. Note that the right-hand side of eqs. 67 and 68 can be expressed in the form of series of $x$ after expansion. The introduction of eqs. 67 and 68 into eq. 66 and the subsequent expansion of the resulting equation give the following equation:

$$
\begin{aligned}
T = {} & [xA^4 + xB^4 + xX^4 + xY^4] + [xA^3B + xAB^3 + \cdots + xBY^3] \\
& + [xA^2B^2 + xA^2X^2 + \cdots + xX^2Y^2] + [xABX^2 + xABY^2 + \cdots + xXYB^2] \\
& + [(xABp^2 + xAB\bar{p}^2) + \cdots + (xXYp^2 + xXY\bar{p}^2)] \\
& + [(\tfrac{1}{2}xA^2p^2 + \tfrac{1}{2}xA^2\bar{p}^2) + \cdots + (\tfrac{1}{2}xY^2p^2 + \tfrac{1}{2}xY^2\bar{p}^2)] + [xp^2\bar{p}^2],
\end{aligned}\tag{69}
$$

where the terms in each pair of brackets represent isomers of the same type.

The terms $xABp^2$ and $xAB\bar{p}^2$ in eq. 69 respectively correspond to **48** and $\overline{\mathbf{48}}$, which are chiral as shown in Fig. 13. Note that **48** and $\overline{\mathbf{48}}$ are not recognized to be enantiomeric, because the variable $s(x^2)$ contained in $a(x)^2 s(x^2)$ (eq. 66) represents the transitivity of two equivalent ligands p and p (or $\bar{p}$ and $\bar{p}$) and does not represent the transitivity between p and $\bar{p}$. Thus, the two chiral isomers (**48** and $\overline{\mathbf{48}}$) are counted separately in place of two diastereomers of pseudoasymmetry (**49** and **50**) to be counted. Hence, the enumeration result is inconsistent with the original purpose of eq. 66 for counting achiral isomers.

Moreover, the terms $\frac{1}{2}xA^2p^2$ and $\frac{1}{2}xA^2\bar{p}^2$ in eq. 69 show the irregularity of the enumeration using eq. 66. Because the terms can be combined into the term $\frac{1}{2}(xA^2p^2 + xA^2\bar{p}^2)$ which is correlated to an enantiomeric pair of chiral isomers, a pair of chiral isomers (**51** and $\overline{\mathbf{51}}$) is counted just once in place of the corresponding achiral *meso*-like isomer (**52**) to be counted. Hence, the enumeration result is again inconsistent with the original purpose of eq. 66 for counting achiral isomers.
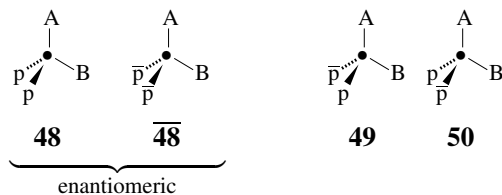
Figure 13: Enantiomeric pair and pseudoasymmetric cases.
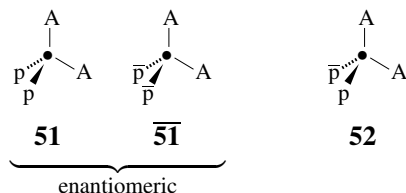


Figure 14: Enantiomeric pair and a *meso*-like case.

It should be emphasized that eq. 69 does not contain terms for representing pseudoasymmetric cases such as $x\mathrm{ABp\overline{p}}$, which correspond to **49** and **50**; nor terms for representing *meso*-like cases such as $x\mathrm{A}^2\mathrm{p\overline{p}}$, which correspond to **52**. These results imply that such pseudoasymmetric cases as **49** and **50** and such *meso*-like cases as **52** are erroneously recognized to be chiral in the treatment by Robinson et al.

On the other hand, the present approach uses eq. 35 and the following ligand inventories:

$$a(x^d) = \mathrm{A}^d + \mathrm{B}^d + \mathrm{X}^d + \mathrm{Y}^d \tag{70}$$

$$c(x^d) = \mathrm{A}^d + \mathrm{B}^d + \mathrm{X}^d + \mathrm{Y}^d + 2\mathrm{p}^{d/2}\overline{\mathrm{p}}^{d/2} \tag{71}$$

$$b(x^d) = \mathrm{A}^d + \mathrm{B}^d + \mathrm{X}^d + \mathrm{Y}^d + \mathrm{p}^d + \overline{\mathrm{p}}^d \tag{72}$$

according to Fujita's proligand method [18–21]. After the introduction of eqs. 70–72 into eq. 35, the resulting equation is expanded to give the following equation:

$$
\begin{aligned}
G =\ & [x\mathrm{A}^4 + x\mathrm{B}^4 + x\mathrm{X}^4 + x\mathrm{Y}^4] + [x\mathrm{A}^3\mathrm{B} + x\mathrm{AB}^3 + \cdots + x\mathrm{BY}^3] \\
& + [x\mathrm{A}^2\mathrm{B}^2 + x\mathrm{A}^2\mathrm{X}^2 + \cdots + x\mathrm{X}^2\mathrm{Y}^2] + [x\mathrm{ABX}^2 + x\mathrm{ABY}^2 + \cdots + x\mathrm{XYB}^2] \\
& + [2x\mathrm{ABp\overline{p}} + 2x\mathrm{AXp\overline{p}} + \cdots + 2x\mathrm{XYp\overline{p}}] \\
& + [x\mathrm{A}^2\mathrm{p\overline{p}} + x\mathrm{B}^2\mathrm{p\overline{p}} + x\mathrm{X}^2\mathrm{p\overline{p}} + x\mathrm{Y}^2\mathrm{p\overline{p}}] + [x\mathrm{p}^2\overline{\mathrm{p}}^2].
\end{aligned} \tag{73}
$$

This equation does not contain terms for representing chiral isomers such as the terms $x\mathrm{ABp}^2$ (or $x\mathrm{AB\overline{p}}^2$) and $\frac{1}{2}x\mathrm{A}^2\mathrm{p}^2$ (or $\frac{1}{2}x\mathrm{A}^2\overline{\mathrm{p}}^2$). Moreover, it correctly contains terms for representing such pseudoasymmetric cases as $x\mathrm{ABp\overline{p}}$, which correspond to **49** and **50**, as well as terms for representing such *meso*-like cases as $x\mathrm{A}^2\mathrm{p\overline{p}}$, which corresponds to **52**. Note that the component $c(x^2)$ contained in $a(x)^2 c(x^2)$ (eq. 35) represents the transitivity between p and $\overline{\mathrm{p}}$ so that **49** (or **50** or **52**) is recognized to be achiral. The enantiomeric pair of p and $\overline{\mathrm{p}}$ satisfies the enantiosphericity characterized by the SI $c_2$ through the component $c(x^2)$.

To emphasize the difference between $T$ (eq. 69) and $G$ (eq. 73), we calculate the subtraction $G - T$ as follows:

$$
\begin{aligned}
G - T &= \quad [2x\text{ABp}\overline{\text{p}} + 2x\text{AXp}\overline{\text{p}} + \cdots + 2x\text{XYp}\overline{\text{p}}] \\
&\quad - [(x\text{ABp}^2 + x\text{AB}\overline{\text{p}}^2) + \cdots + (x\text{XYp}^2 + x\text{XY}\overline{\text{p}}^2)] \\
&\quad + [x\text{A}^2\text{p}\overline{\text{p}} + x\text{B}^2\text{p}\overline{\text{p}} + x\text{X}^2\text{p}\overline{\text{p}} + x\text{Y}^2\text{p}\overline{\text{p}}] \\
&\quad - [(\tfrac{1}{2}x\text{A}^2\text{p}^2 + \tfrac{1}{2}x\text{A}^2\overline{\text{p}}^2) + \cdots + (\tfrac{1}{2}x\text{Y}^2\text{p}^2 + \tfrac{1}{2}x\text{Y}^2\overline{\text{p}}^2)].
\end{aligned}
\tag{74}
$$

The first and second lines of the right-hand side of eq. 74 indicate the correspondence between the term $2x\text{ABp}\overline{\text{p}}$ and the combined term $(x\text{ABp}^2 + x\text{AB}\overline{\text{p}}^2)$ and so on. Obviously, the term $2x\text{ABp}\overline{\text{p}}$ for representing pseudoasymmetric cases (**49** and **50**) becomes equal to the combined term $(x\text{ABp}^2 + x\text{AB}\overline{\text{p}}^2)$ for representing **48** and $\overline{\textbf{48}}$ (cf. Fig. 13), only if their carbon contents alone are taken into consideration. The same situation holds true for the third and fourth lines of the right-hand side of eq. 74, which indicate the correspondence between the term $x\text{A}^2\text{p}\overline{\text{p}}$ and the combined term $\tfrac{1}{2}(x\text{A}^2\text{p}^2 + x\text{A}^2\overline{\text{p}}^2)$ and so on (cf. Fig. 14). In fact, we can obtain $G - T = 0$ by putting $\text{p} = \overline{\text{p}} = x^n$ in eq. 74. This is directly confirmed by examining eqs. 71 and 72, which can be equalized to eq. 68 (i.e., $c(x^d) = b(x^d) = s(x^d)$) because the relationship $\text{p} = \overline{\text{p}}$ results in $2\text{p}^{d/2}\overline{\text{p}}^{d/2} = \text{p}^d + \overline{\text{p}}^d$.

In conclusion, the treatment of Robinson et al. [27] was based on the presumption that such terms as $2x\text{ABp}\overline{\text{p}}$ can be equalized to such combined terms as $(x\text{ABp}^2 + x\text{AB}\overline{\text{p}}^2)$. In other words, their approach enumerates the two enantiomers (**48** and $\overline{\textbf{48}}$) separately in place of the two diastereomers of pseudoasymmetry (**49** and **50**). It follows that their approach took no account of the sphericity concept, although their calculation results up to carbon content 14 were fortunately identical with the present results except some typesetting errors.

# 7 Conclusion

Alkanes are counted as 3D-trees or stereoisomers by means of Fujita's proligand method [18–20]. By starting from enumeration of alkyl ligands as planted 3D-trees, their substitution on a tetrahedral skeleton of $\mathbf{T}_d$-symmetry is examined to generate uninuclear 3D-trees; at the same time, their substitution on a binuclear skeleton of $\mathbf{D}_{\infty h}$-symmetry is examined to generate binuclear 3D-trees. They are enumerated by using functional equations derived from cycle indices with chirality fittingness (CI-CFs), where the functions $a(x^d)$, $c(x^d)$, and $b(x^d)$ (or their modifications) are substituted for three kinds of sphericity indices (SIs), i.e., $a_d$ for homospheric cycles, $c_d$ for enantiospheric cycles, and $b_d$ for hemispheric cycles. The values for binuclear 3D-trees are regarded as contaminants in the enumeration of uninuclear 3D-trees so that the subtraction of the contaminants from the latter enumeration leaves unbalanced 3D-trees to be counted. The enumeration of balanced 3D-trees is conducted distinctly by using the binuclear skeleton of $\mathbf{D}_{\infty h}$-symmetry. After the derivation of respective functional equations for counting alkanes as well as for itemizing them into achiral and chiral ones, they are programmed by means of the Maple programming language and executed up to carbon content 100.

# References

[1] G. Pólya, *Acta Math.*, **68**, 145–254 (1937).

[2] G. Pólya and R. C. Read, "Combinatorial Enumeration of Groups, Graphs, and Chemical Compounds," Springer-Verlag, New York (1987).

[3] H. Hosoya, *Kagaku no Ryoiki*, **26**, 989–1001 (1972).

[4] D. H. Rouvray, *Chem. Soc. Rev.*, **3**, 355–372 (1974).

[5] O. E. Polansky, *MATCH Commun. Math. Comput. Chem.*, **1**, 11–31 (1975).

[6] K. Balasubramanian, *Chem. Rev.*, **85**, 599–618 (1985).

[7] F. Harary, "Graph Theory," Addison-Wesley, Reading (1969).

[8] A. T. Balaban, ed., "Chemical Applications of Graph Theory," Academic Press, London (1976).

[9] N. L. Biggs, E. K. Lloyd, and R. J. Wilson, "Graph Theory 1736–1936," Oxford Univ. Press, Oxford (1976).

[10] G. Pólya, R. E. Tarjan, and D. R. Woods, "Notes on Introductory Combinatorics," Birkhäuser, Boston (1983).

[11] N. Trinajstić, "Chemical Graph Theory, Vol. I and II," CRC Press, Boca Raton (1983).

[12] S. Fujita, "Symmetry and Combinatorial Enumeration in Chemistry," Springer-Verlag, Berlin-Heidelberg (1991).

[13] S. Fujita, *Theor. Chem. Acta*, **91**, 315–332 (1995).

[14] S. Fujita, *Theor. Chem. Acc.*, **99**, 224–230 (1998).

[15] S. Fujita, *Bull. Chem. Soc. Jpn.*, **72**, 2403–2407 (1999).

[16] S. Fujita, *Bull. Chem. Soc. Jpn.*, **73**, 329–339 (2000).

[17] S. Fujita, *J. Math. Chem.*, **30**, 249–270 (2001).

[18] S. Fujita, *Theor. Chem. Acc.*, **113**, 73–79 (2005).

[19] S. Fujita, *Theor. Chem. Acc.*, **113**, 80–86 (2005).

[20] S. Fujita, *Theor. Chem. Acc.*, **115**, 37–53 (2006).

[21] S. Fujita, *MATCH Commun. Math. Comput. Chem.*, **57**, 5–48 (2007).

[22] A. Cayley, *Philos. Mag.*, **47**, 444–446 (1874).

[23] A. Cayley, *Rep. Brit. Assoc. Advance. Sci.*, **45**, 257–305 (1875).

[24] H. R. Henze and C. M. Blair, *J. Am. Chem. Soc.*, **53**, 3042–3046 (1931).

[25] H. R. Henze and C. M. Blair, *J. Am. Chem. Soc.*, **53**, 3077–3085 (1931).

[26] R. Otter, *Ann. Math.*, **49**, 583–599 (1948).

[27] R. W. Robinson, F. Harary, and A. T. Balaban, *Tetrahedron*, **32**, 355–361 (1976).

[28] C. Jordan, *J. Reine Angew. Math.*, **70**, 185–190 (1869).